Article
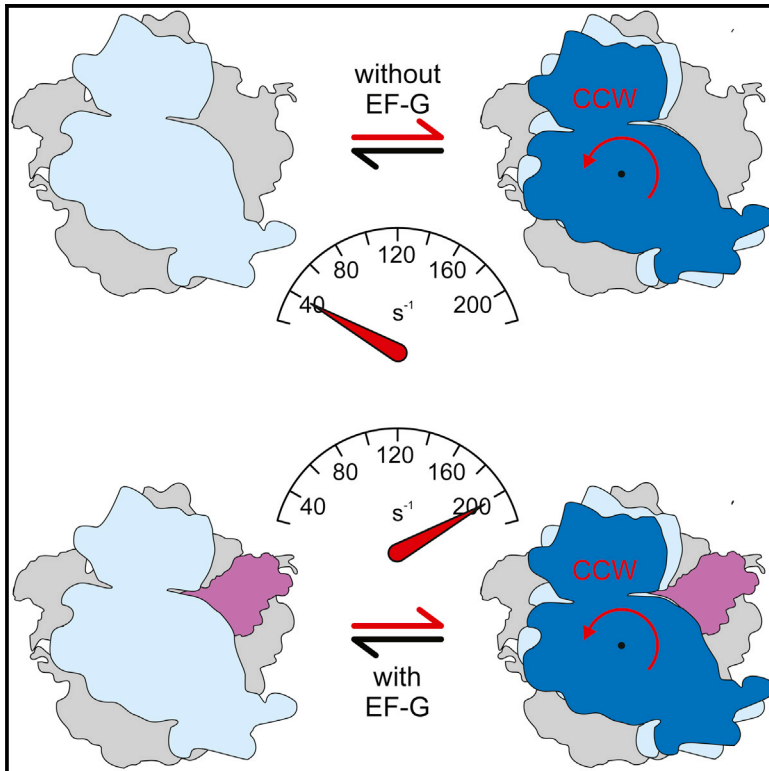
Kinetics of Spontaneous and EF-G-Accelerated Rotation of Ribosomal Subunits

Graphical Abstract

Authors

Heena Sharma, Sarah Adio,
Tamara Senyushkina,
Riccardo Belardinelli, Frank Peske,
Marina V. Rodnina

Correspondence

rodnina@mpibpc.mpg.de

In Brief

Sharma et al. show that spontaneous rotation of the ribosomal subunits after peptide bond formation is strongly accelerated by the recruitment of elongation factor G to the ribosome. The rotated state of the ribosome is an essential, but not rate-limiting, intermediate of translation.

Highlights

- Ribosomal subunits rotate with a constant speed after peptide bond formation

- EF-G recruitment to the ribosome accelerates spontaneous subunit rotation

- Subunit rotation is not rate limiting for EF-G-induced tRNA-mRNA translocation

CellPress

OPEN
ACCESS

Cell Reports
Article

CellPress

Kinetics of Spontaneous and EF-G-Accelerated Rotation of Ribosomal Subunits

Heena Sharma,[1] Sarah Adio,[1] Tamara Senyushkina,[1] Riccardo Belardinelli,[1] Frank Peske,[1] and Marina V. Rodnina[1,2,*]
[1]Department of Physical Biochemistry, Max Planck Institute for Biophysical Chemistry, 37077 Göttingen, Germany
[2]Lead Contact
*Correspondence: rodnina@mpibpc.mpg.de
http://dx.doi.org/10.1016/j.celrep.2016.07.051

SUMMARY

Ribosome dynamics play an important role in translation. The rotation of the ribosomal subunits relative to one another is essential for tRNA-mRNA translocation. An important unresolved question is whether subunit rotation limits the rate of translocation. Here, we monitor subunit rotation relative to peptide bond formation and translocation using ensemble kinetics and single-molecule FRET. We observe that spontaneous forward subunit rotation occurs at a rate of 40 s^{-1}, independent of the rate of preceding peptide bond formation. Elongation factor G (EF-G) accelerates forward subunit rotation to 200 s^{-1}. tRNA-mRNA movement is much slower (10–40 s^{-1}), suggesting that forward subunit rotation does not limit the rate of translocation. The transition back to the non-rotated state of the ribosome kinetically coincides with tRNA-mRNA movement. Thus, large-scale movements of the ribosome are intrinsically rapid and gated by its ligands such as EF-G and tRNA.

INTRODUCTION

Translation elongation involves repetitive cycles of mRNA decoding, peptide bond formation, and tRNA-mRNA translocation, which result in a forward movement of the ribosome along the mRNA as the nascent peptide is elongated. Translocation is a critical point in reading frame maintenance and is a target for a variety of antibiotics that attack bacterial and fungal cells, which underscores the importance of the process. The translocation step entails coordinated movements of the ribosomal subunits and of the two tRNA molecules together with the mRNA and is promoted by EF-G–GTP. Each time a peptide bond is formed, the small ribosomal subunit (SSU) rotates spontaneously in counterclockwise (CCW) direction relative to the large ribosomal subunit (LSU) from the non-rotated (N) to the rotated (R) state of the pre-translocation (PRE) complex (Agirrezabala et al., 2008; Cornish et al., 2008; Ermolenko et al., 2007a; Frank and Agrawal, 2000; Julián et al., 2008; Zhang et al., 2009) (Figure S1A). The transitions between the N and R states due to alternating CCW and clockwise (CW) movements of the ribosomal subunits

provide a signature of ongoing translation (Aitken and Puglisi, 2010; Chen et al., 2013a; Marshall et al., 2008). The acceptor arms of the peptidyl-tRNA and deacylated tRNA move from their classical (C) positions in the A and P sites, respectively, to hybrid (H) states in which the tRNA acceptor ends have moved toward the P and E sites on the LSU, while the anticodon arms of the two tRNAs remain in the A and P sites on the SSU (Agirrezabala et al., 2008; Blanchard et al., 2004; Dunkle et al., 2011; Fischer et al., 2010; Moazed and Noller, 1989; Valle et al., 2003). The two macro-states, C and H, entail a number of sub-states that differ with respect to the exact position of the tRNAs and the degree of subunit rotation (Fischer et al., 2010; Holtkamp et al., 2014; Munro et al., 2007; Pan et al., 2007; Zhang et al., 2009). Ribosomal protein L1 changes its position from open (L1$_{open}$) to closed (L1$_{closed}$) relative to the tRNA in the P/E state (Chen et al., 2013b; Cornish et al., 2009; Fei et al., 2009; Fei et al., 2008; Munro et al., 2010a, 2010b; Valle et al., 2003). The three types of fluctuations—N ↔ R, C ↔ H, and L1$_{open}$ ↔ L1$_{closed}$— are loosely coupled (Fischer et al., 2010) and have somewhat different fluctuation kinetics (Munro et al., 2010a; Wasserman et al., 2016). Biochemical and ensemble kinetics experiments demonstrated that the R-H state (that is, the conformation of the ribosome with ribosomal subunits in the rotated state and tRNAs in hybrid states) is an authentic translocation intermediates that serves to accelerate tRNA movement through the ribosome (Dorner et al., 2006; Horan and Noller, 2007; Semenkov et al., 2000). Binding of EF-G–GTP to the ribosome stops the fluctuations of L1, stabilizes the R-H state and induces the formation of yet another subset of conformations, the chimeric (CHI) or intermediate (INT) states (Adio et al., 2015; Brilot et al., 2013; Ramrath et al., 2013; Ratje et al., 2010; Wasserman et al., 2016; Zhou et al., 2013, 2014). GTP hydrolysis by EF-G promotes rapid movement of the tRNA-mRNAs complex into the post-translocation (POST) state accompanied by CW rotation of the ribosomal subunits into the N state (Belardinelli et al., 2016; Ermolenko and Noller, 2011; Rodnina et al., 1997; Wasserman et al., 2016).

Spontaneous fluctuations between C and H or N and R states were studied by single-molecule fluorescence resonance energy transfer FRET (smFRET) methods (Note S1 and references therein). Estimations based on smFRET measurements indicated that the spontaneous transitions toward the R-H-L1$_{closed}$ states are rather slow, in the range from 0.05 s^{-1} to 10 s^{-1} (Cornish et al., 2008; Fei et al., 2008; Kim et al., 2007; Munro et al., 2010a; Wasserman et al., 2016) (Note S1; Table S2). These rates

are either slower or in the same range as the rates of tRNA translocation measured by ensemble kinetics and smFRET (Chen et al., 2011; Holtkamp et al., 2014; Pan et al., 2007). The effect of EF-G on this transition is difficult to estimate, because EF-G binding to PRE complexes induces rapid transition toward CHI and POST states. To overcome this limitation, the rates of the transitions toward the R-H-L1$_{closed}$ state were estimated on translocationally inactive complexes, i.e., without a tRNA in the A site. Also in the presence of EF-G, these rates are low and comparable to the translocation rates. These results implied that the rate of spontaneous fluctuations preceding EF-G binding may determine the global rate of EF-G binding and translocation (Munro et al., 2010a; Wang et al., 2011; Wasserman et al., 2016). In contrast, ensemble kinetics hinted at a possibility that in the presence of EF-G the N-to-R rotation rate of a PRE complex is very high (>200 s^{-1}), although the exact rates were not determined and the rates of spontaneous fluctuations were not measured (Ermolenko and Noller, 2011; Guo and Noller, 2012). We note that it is important to study translocation on true PRE complexes with a deacylated tRNA in the P site and a peptidyl-tRNA in the A site, because the presence of an A site tRNA, or at least its anticodon–stem loop domain, is essential for translocation (Joseph and Noller, 1998) and the rate of translocation depends on the acylation state of the tRNAs (Semenkov et al., 2000). Furthermore, the rates of subunit rotations were mostly measured at conditions dictated by smFRET experiments, typically at 20°C–25°C and with buffers containing high Mg^{2+} or polyamine concentrations, rather than at conditions optimal for translation (Note S1). Surprisingly, although peptide bond formation was proposed to drive CCW rotation, no experiments have been reported that compare the rates of the two reactions. The lack of information on the relative rates of peptide bond formation, CCW and CW subunit rotation, and tRNA translocation at conditions of rapid and efficient translation is a major source of ambiguity in the understanding of the mechanism of translocation. This prompted us to re-examine the kinetics of spontaneous and EF-G-induced subunit rotation in the context of peptide bond formation and translocation. We determined the rates of peptide bond formation and translocation for different tRNA pairs by quench flow and followed spontaneous R state formation by ensemble kinetics and smFRET using an established FRET pair for monitoring subunit rotation. We then asked whether EF-G–GTP binding modulates the rates of the CCW rotation. Finally, we compared the rates of CCW and CW rotations and tRNA translocation measured at 37°C and 22°C and various buffer conditions. We show that EF-G binding substantially accelerates CCW rotation, such that it becomes much faster than tRNA–mRNA translocation, whereas CW rotation is concomitant with translocation. The data provide an important insight into the contribution of an authentic early on-pathway conformational rearrangement to the energetics of translocation.

RESULTS

Experimental Approach

To follow the rotation of the SSU relative to the LSU, we used the FRET assay developed and validated by Noller, Clegg, and colleagues (Cornish et al., 2008; Ermolenko et al., 2007a, 2007b,

2013; Ermolenko and Noller, 2011; Hickerson et al., 2005; Ling and Ermolenko, 2015; Majumdar et al., 2005). We attached fluorophores to ribosomal proteins bS6 and bL9 (Experimental Procedures). For ensemble experiments, bS6 was labeled with Alexa 488, serving as FRET donor, and bL9 was labeled with the acceptor dye Alexa 568 (Ermolenko et al., 2007a; Ermolenko and Noller, 2011). For smFRET experiments, bS6 was labeled with Cy5 and bL9 with Cy3 (Cornish et al., 2008; Qin et al., 2014). The functional activity of the ribosomes was not changed by labeling, as verified by their unaltered ability to bind tRNAs and the unaffected rate of translocation, as assessed by time-resolved puromycin (Pmn) assay (Figure S1B).

As shown previously (Belardinelli et al., 2016; Ermolenko et al., 2007a; Ermolenko and Noller, 2011), subunit rotations result in FRET changes between the S6-labeled SSU and L9-labeled LSU. FRET causes a decrease of donor fluorescence and a concomitant increase of acceptor fluorescence of the S6-L9 FRET pair (Belardinelli et al., 2016); for the ensemble kinetics, we used the changes in the acceptor fluorescence to monitor changes in FRET efficiency. The acceptor fluorescence decreases upon addition of the ternary complex, EF-Tu–GTP–Phe-tRNA^{Phe}, to the S6-L9 double-labeled initiation complex, 70S-mRNA-fMet-tRNA^{fMet}, indicating subunit rotation. Addition of EF-G–GTP to the resulting PRE complex causes tRNA translocation; fluorescence increases to the initial value (Figure S1C). Fluorescence does not change when the PRE complex is mixed with buffer in the absence of EF-G (Figure S1D). The fluorescence anisotropy of the FRET donor, as measured on single-labeled ribosomes, is rather low (0.197 ± 0.003), indicating sufficiently high mobility of the fluorophore to assume an orientation factor κ^2 close to 2/3 (Majumdar et al., 2005). For the acceptor fluorophore, the anisotropy is higher (0.292 ± 0.002), which, however, does not compromise the interpretation of FRET changes in terms of distance changes (Ermolenko et al., 2007a; Majumdar et al., 2005). These and other controls for the photophysical effects of the double-labeled ribosomes suggest that the observed changes in FRET can be interpreted in terms of distance changes between the two reporter groups (Ermolenko et al., 2007a; Hickerson et al., 2005; Majumdar et al., 2005).

Spontaneous CCW Subunit Rotation with Different tRNAs in the P Site

We first measured the rates of peptide bond formation and spontaneous CCW rotation by quench flow and stopped flow, respectively (Figures 1A and 1B). We prepared POST complexes with different dipeptidyl-tRNAs in the P site (fMetX-tRNA^X, where X is Lys, Val, Phe, or Pro, in the following denoted as fMX) and rapidly mixed them with Pmn. Initially, we used Pmn as an A-site substrate instead of native aminoacyl-tRNAs (aa-tRNA), because Pmn binding and accommodation are not rate limiting for peptide bond formation (Sievers et al., 2004), and thus the kinetics of peptide bond formation depends solely on the P-site peptidyl-tRNA. The Pmn reaction is rapid with fMK, fMV, and fMF and very slow with fMP (Figure 1A), in agreement with previous observations (Wohlgemuth et al., 2008). The subsequent CCW rotation, which was monitored as a fluorescence decrease, followed the same tendency (Figure 1B), with the apparent rate constants (k$_{app}$) being generally lower than those of peptide
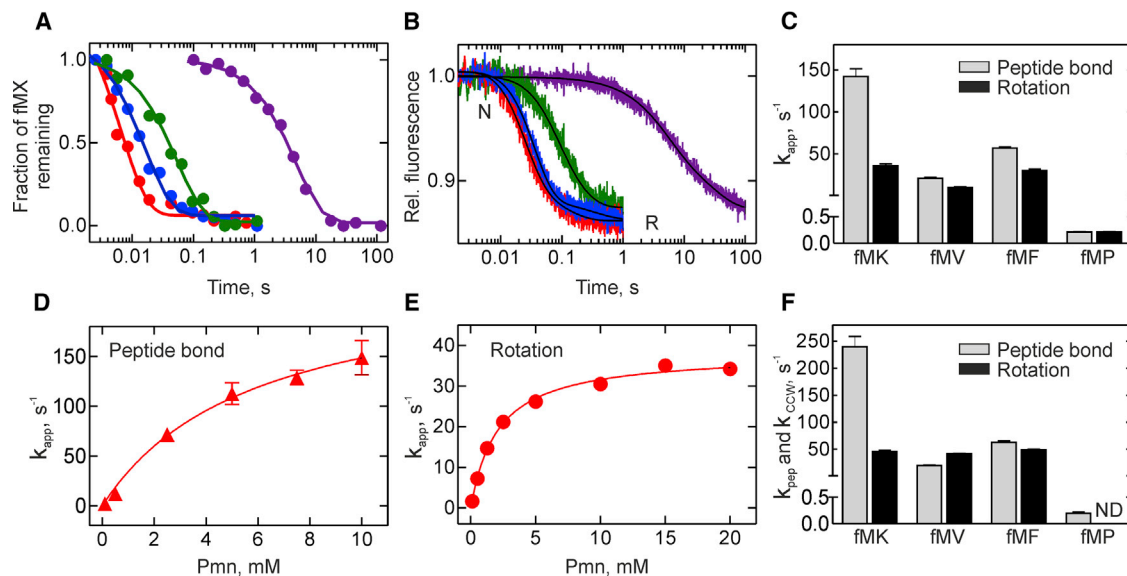
Figure 1. CCW Rotation upon Reaction of Different P-Site Peptidyl-tRNAs with Pmn

(A) Time courses of peptide bond formation. POST complexes with fMetX-tRNA^X in the P site, where X is Lys (red), Val (green), Phe (blue), or Pro (purple), were rapidly mixed with Pmn (10 mM). Smooth lines represent global fits.

(B) CCW subunit rotation. Color code as in (A); smooth lines are global fits.

(C) The apparent rate constants (k_{app}) of peptide bond formation and subunit rotation obtained by exponential fitting of the data from (A) and (B). Plotted are the k_{app} values of the major step (>80% of the total amplitude).

(D and E) Pmn concentration dependence of peptide bond formation (D) and spontaneous CCW rotation (E) for the fMK complex. Hyperbolic fits yield 240 ± 20 s^{-1} and 40 ± 1 s^{-1} for the rate constants of peptide bond formation (k_{pep}) and CCW rotation (k_{rot}) at saturation, with K_M values of 6 ± 1 mM and 2.0 ± 0.1 mM, respectively. The elemental rate constant (k_{CCW}) of subunit rotation is 48 ± 3 s^{-1} (Supplemental Experimental Procedures).

(F) Elemental rate constants of peptide bond formation (k_{pep}) and subunit rotation (k_{CCW}) obtained by numerical integration analysis of the data from (A) and (B). Values are mean ± SD (n = 3 independent kinetic experiments).

Experiments were carried out in TAKM$_7$ at 37°C. See also Figures S1 and S2.

bond formation (Figure 1C). To determine the elemental rate constant of the CCW rotation, we deconvoluted peptide bond formation and subunit rotation. For this, we used two different approaches. For the fMK POST complex, the K_M value for Pmn is very high, such that the maximum rate of peptide bond formation is not reached even at high Pmn concentration (10 mM) (Wohlgemuth et al., 2008). Therefore, we measured the rates of peptide bond formation and CCW rotation at increasing Pmn concentrations. The rates of peptide bond formation and subunit rotation at saturation with Pmn estimated by hyperbolic fitting are 240 ± 20 s^{-1} and 40 ± 2 s^{-1}, respectively (Figures 1D and 1E). Then, we calculated the elemental rate constant of CCW rotation, k_{CCW} = 48 ± 3 s^{-1}, from these two values (Figure 1F) (Supplemental Experimental Procedures). In contrast to fMK, the K_M values for the Pmn reaction with fMV and fMF are lower, such that a Pmn concentration of 10 mM is sufficient to attain the near-maximum velocities (Wohlgemuth et al., 2008). These values were thus taken as elemental rate constants of peptide bond formation (Figure 1F).

As a second approach, we calculated k_{CCW} values by numerical integration, assuming a sequential two-step model with peptide bond formation followed by CCW subunit rotation; where necessary, another step was added to account for a minor additional fluorescence change (Supplemental Experimental Procedures). We assumed that the subunit rotation was quasi-

irreversible at 37°C in TAKM$_7$, because (1) the y axis intercept of the concentration dependence of the respective k_{app} is close to zero for the fMK complexes (Figure 1E) and (2) there was no variation in the CCW rotation amplitude for different complexes. For fMK, the calculation yielded a value of k_{CCW} = 46 ± 2 s^{-1}, identical to the value obtained from the Pmn titration. For fMV and fMF, the k_{CCW} values were in the same range (40–50 s^{-1}), even though the rates of peptide bond formation varied with the P site tRNA (Figure 1F). For the fMP complex, very slow peptide bond formation limits the CCW rotation; therefore, an accurate value of k_{CCW} could not be determined for that complex.

The rate constants of the spontaneous CCW rotation reported here are at least ten times higher than the values obtained by smFRET (Cornish et al., 2008; Ermolenko et al., 2013; Qin et al., 2014; Wasserman et al., 2016). For better comparison with smFRET results (typically obtained at ~22°C), we determined the rates of subunit rotation at different temperatures (Figure S2A). The Arrhenius plot is linear (Figure S2B), indicating that a single elemental reaction was monitored, and the rate of CCW rotation is ~8 s^{-1} at 22°C. This value is somewhat higher than the values obtained for the same S6-L9 reporter positions with a synthetic analog of peptidyl-tRNA, N-Ac-Phe-tRNA^{Phe}, in the A site (0.3–1.7 s^{-1}) (Cornish et al., 2008; Qin et al., 2014) but in the same range as the values for the PRE complex of the same composition obtained with labels on proteins S13 and
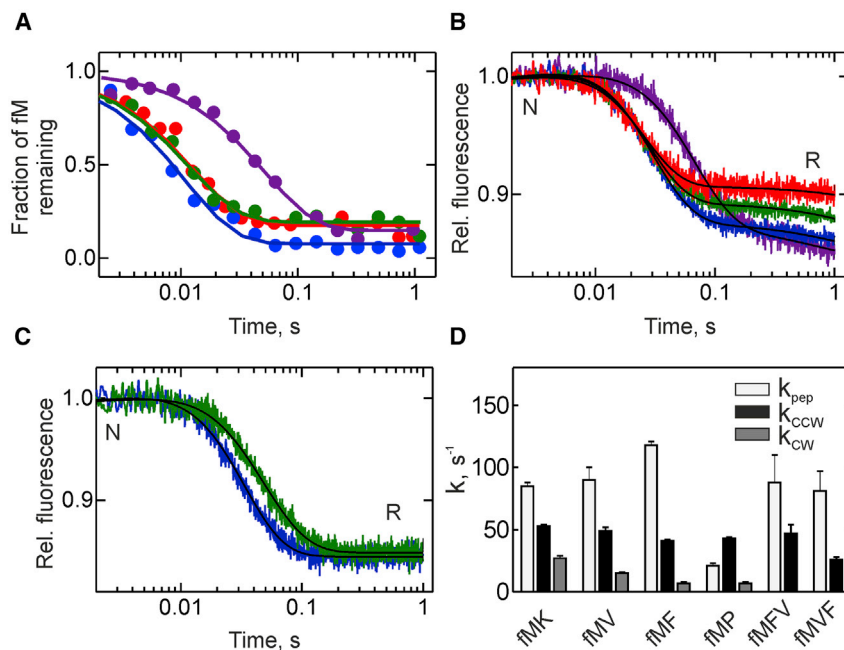
Figure 2. Spontaneous CCW Rotation upon Reaction with Different Aminoacyl-tRNAs

(A) Time courses of peptide bond formation. Initiation complexes were rapidly mixed with ternary complexes EF-Tu-GTP-X-tRNA^X at saturating concentration (10 μM). X is Lys (red), Val (green), Phe (blue), or Pro (purple). Smooth lines represent global fits.

(B) CCW subunits rotation. Color code as in (A); smooth lines represent global fits.

(C) Subunit rotation upon reaction of POST(fMF) (blue) or POST(fMV) (green) complexes with the ternary complex EF-Tu–GTP–Val-tRNA^{Val} or EF-Tu-GTP-Phe-tRNA^{Phe}, respectively, at saturating concentration (10 μM). Smooth lines represent global fits.

(D) The rate constants of accommodation/peptide bond formation (k_{pep}) and the elemental rate constants of subunit rotation (k_{CCW} and k_{CW}) obtained by numerical integration of the data from (A) and (B). Values are mean ± SD (n = 3 independent kinetic experiments).

Experiments were carried out in TAKM$_7$ at 37°C. See also Table 1.

L1 ($\sim$5 s^{-1}) (Wasserman et al., 2016) and comparable to the values we obtained by smFRET (see below).

Spontaneous CCW Rotation of PRE Complexes with Different tRNAs in the A Site

Next, we monitored the kinetics of peptidyl transfer and spontaneous rotation with aa-tRNAs as A-site substrates. We prepared initiation complexes with mRNAs that differed in the second codon and rapidly mixed them with ternary complexes EF-Tu–GTP–X-tRNA^X, where X was Lys, Val, Phe, or Pro (Figure 2). For comparison, we also used complexes carrying either fMetPhe-tRNA^{Phe} (POST(fMF)) or fMetVal-tRNA^{Val} (POST(fMV)) in the P site and mixed them with ternary complexes EF-Tu–GTP–Val-tRNA^{Val} or EF-Tu–GTP–Phe-tRNA^{Phe}, respectively. Rates of peptide bond formation were very similar with Lys-, Val-, and Phe-ternary complexes and much lower with Pro, consistent with the notion that aa-tRNA accommodation is rate limiting for peptide bond formation unless the substrate reacts exceptionally slowly, such as Pro (Wohlgemuth et al., 2008, 2010). While the FRET efficiency generally is decreased by the CCW rotation, the final levels varied depending on the aa-tRNA in the A site (Figure 2B), although the yield of dipeptide formation was not significantly different (Figure 2A). The highest rotation amplitude was observed when POST complexes (fMF or fMV) reacted with the ternary complexes (Figure 2C).

The different amplitudes of the subunit rotation (Figure 2B) may reflect either different proportions of spontaneously formed R and N states or the formation of additional, intermediate rotation states depending on the A-site tRNA. To distinguish between these alternatives, we determined the population distribution of the different complexes by measuring smFRET. In all cases, we found two subpopulations with FRET efficiencies of 0.7 (N state) and 0.5 (R state), but the ratio between the N and

R states depended on the A-site tRNA (Figure 3; Table S1). In the PRE complex with deacylated tRNA^{fMet} in the P site and fMetPhe-tRNA^{Phe} in the A site (PRE(fMF)) the R state was favored. In contrast, the majority of the PRE(fMK) and PRE(fMV) complexes was in the N conformation. Addition of EF-G and translocation converted the ribosomes into the high-FRET POST state, indicating that the majority of the formed POST complexes assumed the N conformation. The rates of subunit rotation (CCW and CW), as calculated from the spontaneous transitions (Figure S3; Table 1), were similar to previously published values (Cornish et al., 2008; Qin et al., 2014; Wasserman et al., 2016).

Given that the spontaneous transition between N and R states is reversible, we sought to determine the rate constants of the spontaneous CCW and CW rotation from the kinetic data (Figure 2). The rates of peptide bond formation measured at saturating concentrations of the ternary complex (10 μM) reflect the rate-limiting step for amino acid incorporation, which in most cases is the accommodation of aa-tRNA in the A site followed by rapid peptide bond formation, except for Pro, where the chemistry is rate limiting (Wohlgemuth et al., 2008, 2010). We determined the rates of CCW and CW rotations by numerical integration, using a three-step sequential model, with the first, irreversible step representing peptide bond formation, a second, reversible step for subunit rotation, and an additional step of unknown origin with a very small amplitude (<10% of the total amplitude) (Supplemental Experimental Procedures). The values were k_{CCW} = 40 s^{-1} to 50 s^{-1} and k_{CW} = 7 s^{-1} to 27 s^{-1}, depending on the tRNAs in the A and P site (Figure 2D; Table 1).

EF-G-Induced Subunit Rotation

We next asked how EF-G–GTP affects subunit rotation (Figures 4A and 4B). We prepared different PRE complexes, as described
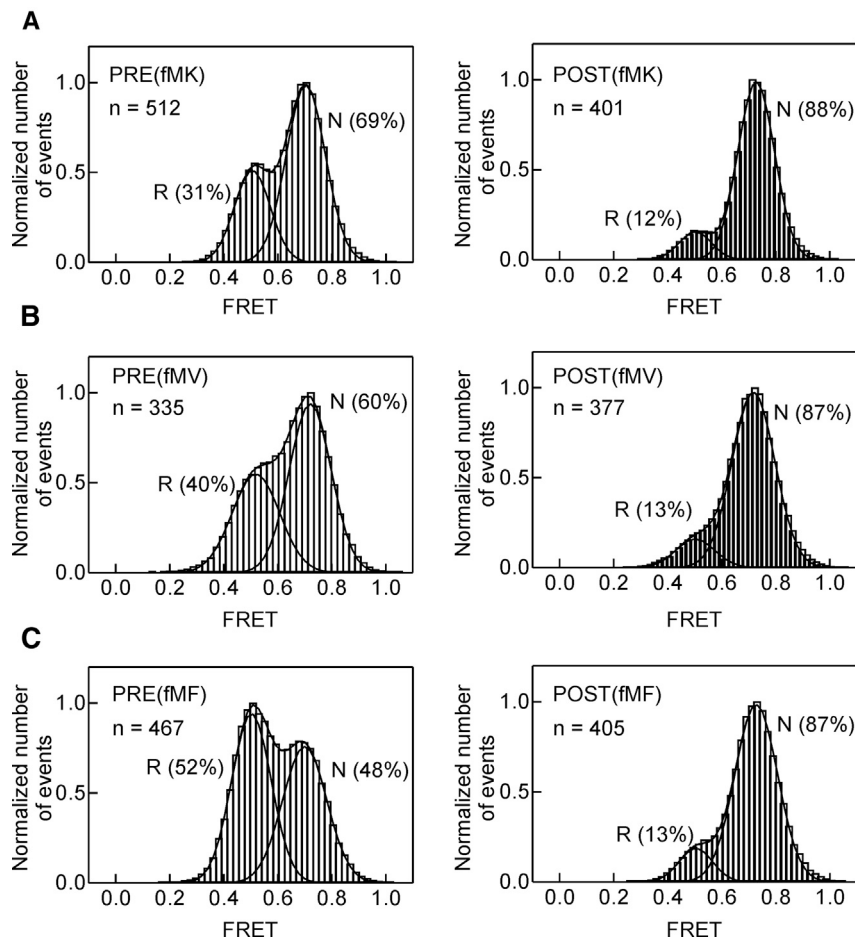
Figure 3. Distribution of N and R States in PRE and POST Complexes Determined by smFRET

PRE complexes contained deacylated tRNA^{fMet} in the P site and fMet-X-tRNA^X in the A site, as indicated in panels (A)–(C). POST complexes contained only fMet-X-tRNA^X in the P site. n is the number of traces analyzed. Experiments were carried out in smFRET buffer at 22°C. See also Figure S3 and Table S1.

rotation (Figure S5). A similar trend was observed at 25°C, in that the rate of CCW rotation was 10 s^{-1} in the absence (Figure S2A) and 50 s^{-1} in the presence of EF-G (Figure S2C), whereas the rate of CW rotation, 4 s^{-1} (Figure S2D), was similar to the rate of tRNA movement, which was 2 s^{-1} (Figure S4; Table 2). These results suggest that EF-G accelerates the CCW rotation by a factor of five compared to the spontaneous rotation and that tRNA movement is much slower (by ~20- fold) than EF-G-induced CCW rotation.

To further correlate results from ensemble kinetics and smFRET we also monitored the kinetics of EF-G-promoted subunit rotation at smFRET buffer and temperature conditions (Figure 4B). For PRE(fMK) and PRE(fMV), a downward CCW rotation phase was well resolved from the subsequent CW rotation. From the amplitude ratio of the CCW phase and the overall R-to-N transition, we could estimate the fraction of PRE complex present in the N state prior to EF-G addition (Table S1). The fraction of the N state obtained by ensemble kinetics is very close to that obtained from the state distributions in the single-molecule experiments, indicating good agreement between the two approaches. Analogous calculations from the CCW and CW amplitudes of the stopped-flow experiment in TAKM$_7$ at 25°C or 37°C yielded the fraction of complexes in the N state for PRE(fMK) and PRE(fMV) (Figures S2C and S2D; Table S1). For the PRE(fMF) complex, the fraction of the N state was calculated from the intrinsic fluorescence intensity values (Belardinelli et al., 2016).

From the kinetic analysis of subunit rotation at smFRET conditions, rate constants of EF-G-induced CCW rotation, k$_{CCW}$, are ~14 and 12 s^{-1} for PRE(fMK) and PRE(fMV), which is much higher than the rate constant of the CW rotation, k$_{CW}$, and translocation, k$_{TL}$, 1.2 s^{-1} and 0.5 s^{-1}, for PRE(fMK) and PRE(fMV) (Table 2). In comparison to PRE(fMK) and PRE(fMV) complexes, the time course of subunit rotation in the PRE(fMF) complex does not entail a CCW phase, even though 47% of the PRE complexes are expected to be in the N state. The kinetic analysis of translocation suggested that in the PRE(fMF) complex, CCW rotation coincides with the initial EF-G binding step (Belardinelli et al., 2016). It is thus likely that at the high EF-G concentration used in these experiments, the rate of CCW rotation is too high to

above, and mixed them with EF-G–GTP at saturating concentration. For PRE(fMK) and PRE(fMV), a downward phase, which reflects CCW rotation, is followed by an upward phase, reporting CW rotation taking place upon translocation (Ermolenko and Noller, 2011) (Figure 4A). For PRE(fMF) and PRE(fMP), the downward amplitude was very small and the upward phase started after a delay and proceeded with similar kinetics for all PRE complexes studied. The complete analysis of translocation kinetics with PRE(fMF) indicated that the delay phase comprised a small downward phase followed by an upward phase that cancelled out the signal change (Belardinelli et al., 2016); thus, the analysis by exponential fitting was very difficult in this case. In contrast, FRET changes with PRE(fMK) or PRE(fMV) are amenable for analysis by exponential fitting. The dependence on the EF-G concentration yields rate constants of CCW rotation (k$_{CCW}$) of 200 ± 20 s^{-1} or 210 ± 10 s^{-1} and of CW rotation (k$_{CW}$) of 15 ± 1 s^{-1} or 11 ± 1 s^{-1} for PRE(fMK) or PRE(fMV), respectively (Figures 4C and 4D). The rates of tRNA movement, as measured with the time-resolved Pmn assay, were 12 ± 2 s^{-1} (37°C) for both fMK and fMV (Figure S4; Table 2), i.e., almost identical to the rates of CW rotation. CW rotation and tRNA movement are coupled, because blocking or slowing down of tRNA movement by replacing GTP with a non-hydrolyzable GTP analog, or using a slowly translocating EF-G mutant, impairs CW, but not CCW,

Table 1. Rates of Spontaneous N-to-R and R-to-N Transitions Determined by smFRET and Ensemble Kinetics

	Experimental Conditions			
	smFRET, 22°C		TAKM$_7$, 37°C[a]	
	k_{CCW}, s^{-1}	k_{CW}, s^{-1}	k_{CCW}, s^{-1}	k_{CW}, s^{-1}
PRE	N → R	R → N	N → R	R → N
fMK (320)[b]	2.1 ± 0.1 (3,557)[c]	3.7 ± 0.1 (3,561)[c]	53 ± 1	27 ± 2
fMV (141)[b]	3.2 ± 0.3 (1,153)[c]	3.9 ± 0.4 (1,168)[c]	49 ± 3	15 ± 1
fMF (196)[b]	4.1 ± 0.2 (1,768)[c]	3.0 ± 0.2 (1,757)[c]	41 ± 1	7 ± 1

N is the population in high-FRET state (FRET efficiency = 0.7); R is the population in low-FRET state (FRET efficiency = 0.5). All values are mean ± SD from three independent datasets. See also Figure S3 and Table S1.
[a]Rates calculated from numerical integration analysis of data in Figure 2.
[b]The number of dynamic traces used to calculate the transition rates between the two populations in smFRET experiments.
[c]The number of transitions observed in smFRET experiments.

be monitored even with a stopped-flow instrument. The CW rotation of the PRE(fMF) complex was at least biphasic, with apparent rate constants of 11 s^{-1} and 0.5 s^{-1}, consistent with a multistep mechanism of translocation (Belardinelli et al., 2016; Wasserman et al., 2016). Thus, at all conditions studied, EF-G accelerates the CCW rotation on the fraction of the PRE complexes that remained in the N state after peptide bond formation, such that the N-to-R transition becomes much faster than the subsequent translocation and CW rotation steps.

DISCUSSION

In the present study we determined the rates of spontaneous and EF-G-induced subunit rotation by ensemble kinetics and compared them to those of peptide bond formation and translocation. In principle, the peptidyl transfer reaction may promote subunit rotation by forming a deacylated tRNA in the P site and a peptidyl-tRNA in the A site, which are prone to form H states and may thus favor subunit rotation for structural reasons (Blanchard et al., 2004; Cornish et al., 2008; Kim et al., 2007; Munro et al., 2007). Alternatively, the energy of peptide bond formation may be directly utilized to drive CCW subunit rotation (Marshall et al., 2008). We find that at 37°C, the rate of spontaneous CCW rotation k_{CCW} is ~40 s^{-1} with a number of different tRNAs in P and A sites independent of the rate of peptide bond formation. The k_{CCW} values measured at smFRET conditions (22°C) for PRE complexes formed as a result of peptide bond formation (Table 1) or without peptide bond formation by direct binding of a peptidyl-tRNA analog, N-Ac-Phe-tRNA^{Phe}, into the A site (Qin et al., 2014) are not grossly different, indicating that the energy of peptide bond formation is not utilized to drive the subunit rotation. Furthermore, our data support the notion that spontaneous fluctuations in the PRE complex are reversible (Cornish et al., 2008; Fei et al., 2008; Munro et al., 2007; Wasserman et al., 2016). We find that the rate of the spontaneous N-to-R rotation is independent of tRNA, whereas the rate of R-to-N rota-

tion depends on the tRNA in the PRE complex and defines the equilibrium between N and R states. The fraction of complexes in the N state ranges from 0.1 to 0.4 at conditions of rapid translation and increases at conditions typically used in smFRET measurements. These findings are consistent with other smFRET and structural studies, as well as molecular dynamic simulations that report the existence of largely iso-energetic fluctuating ribosome populations corresponding to the different subunit rotational states and tRNA and L1 positions. Thus, we conclude that peptide bond formation has a structural, rather than an energetic, effect on subunit rotation; the thermal energy is sufficient to power the spontaneous fluctuations of the PRE complex between the rotational states.

Upon initial binding to the ribosome, EF-G stabilizes the R-H-L1$_{closed}$ state by halting backward fluctuations toward the N-C-L1$_{open}$ state (Adio et al., 2015; Chen et al., 2011; Munro et al., 2010a, 2010b, 2010c; Spiegel et al., 2007; Valle et al., 2003). A question that remains controversial is whether EF-G can bind to the N state or requires the N-to-R transition before binding (Munro et al., 2010c; Wasserman et al., 2016). Analysis of the conformational state of the ribosome immediately prior to translocation when monitored by smFRET between tRNA-L11 shows that EF-G can bind to both C and H states (Adio et al., 2015; Chen et al., 2011). Also, ensemble kinetic analysis suggests that changing the fraction of C versus H state in the ribosome population does not affect the rate of GTP hydrolysis by EF-G or of tRNA movement, suggesting that either EF-G can bind to either state or the transition between the N and R states is rapid (Holtkamp et al., 2014; Rodnina et al., 1997; Walker et al., 2008). Furthermore, two recent structures show EF-G bound to the ribosome in the N state (Li et al., 2015; Lin et al., 2015). These structures, together with the smFRET and ensemble kinetics, provide strong evidence that EF-G can bind to either the N-C or R-H state and engages in translocation via a transient N-to-R rotation with concomitant stabilization of the R-H state.

One major challenge in dissecting the mechanism of translocation is to estimate the effect of EF-G on the rates of N-to-R transitions. This is because binding of EF-G induces rapid progression of the PRE complex through translocation intermediates until the POST state is reached. Experiments with ribosome complexes that do not translocate (i.e., with the vacant A site) suggest that EF-G accelerates the L1 closure by a factor of six to eight to a rate of up to 3 s^{-1} (Fei et al., 2009; Munro et al., 2010b). When subunit rotation is monitored using the S6-L9 reporter pair on the ribosomes with a vacant A site, the effect is two-fold (to 1.2 s^{-1}) (Cornish et al., 2008). Here, we show that EF-G–GTP-induced CCW rotation on the fraction of PRE complexes that have remained in the N state after peptide bond formation is extremely fast (200 s^{-1}) (Figure 5). EF-G accelerates the CCW subunit rotation to a similar extent for different tRNAs or experimental conditions (i.e., approximately five-fold compared to spontaneous rotation). This acceleration was not observed in previous smFRET experiments, either because the reaction is too fast for the time resolution of conventional smFRET experiments or because CCW rotation is obscured by subsequent translocation events (Chen et al., 2013a; Cornish et al., 2008; Wasserman et al., 2016). On the other hand, our results are consistent with ensemble kinetic experiments (performed at 22°C), which noted
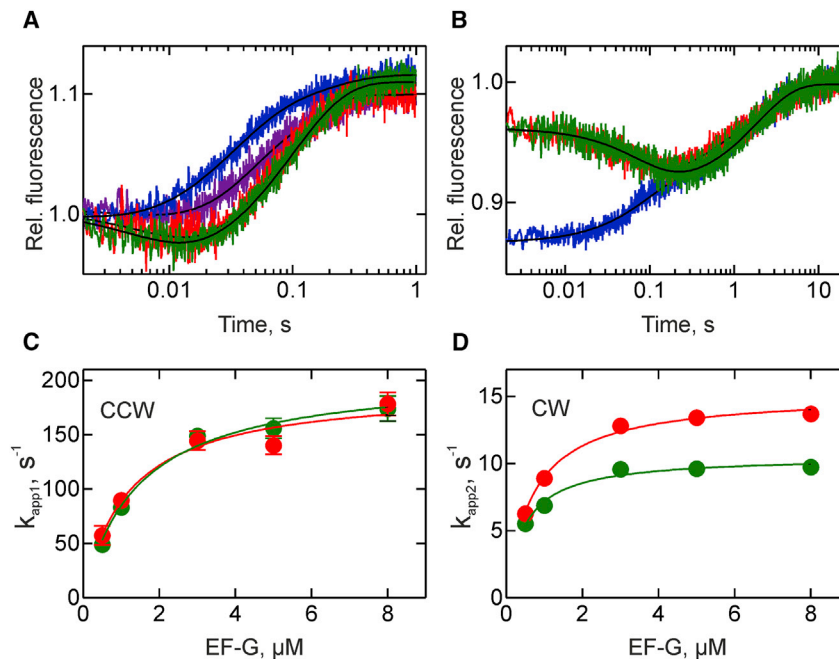
Figure 4. EF-G-Induced Subunit Rotation

(A) Subunit rotation upon addition of EF-G–GTP to PRE complexes with fMetX-tRNA^X in the A site, where X is Lys (red), Val (green), Phe (blue), or Pro (purple) in TAKM$_7$ at 37°C. Smooth lines are two-exponential fits.

(B) Same as (A) in smFRET buffer at 22°C.

(C and D) Concentration dependence. Apparent rate constants of CCW (k_{app1}) and CW (k_{app2}) subunit rotation upon translocation with Lys (red) and Val (green) complexes at 37°C in TAKM$_7$. Hyperbolic fits yield rate constants for CCW rotation of 200 ± 20 s^{-1} ($K_M = 1.2 \pm 0.4$ μM) for PRE(fMK) and 210 ± 10 s^{-1} ($K_M = 1.4 \pm 0.2$ μM) for PRE(fMV). The rate constants of CW rotation are 15 ± 1 s^{-1} ($K_M = 0.7 \pm 0.1$ μM) and 11 ± 1 s^{-1} ($K_M = 0.5 \pm 0.1$ μM), respectively.

See also Figures S2 and S4.

a very rapid CCW rotation upon EF-G–GTP addition to a PRE complex with N-Ac-Phe-tRNA^{Phe} in the A site (Ermolenko and Noller, 2011). Likewise, our recent translocation experiments with the PRE(fMF) complex and EF-G–GTPγS revealed a very rapid CCW subunit rotation upon EF-G binding preceding tRNA translocation (Belardinelli et al., 2016). In comparison to CCW subunit rotation, CW rotation and tRNA translocation are largely concomitant, but much slower, steps (Belardinelli et al., 2016; Ermolenko and Noller, 2011). CW rotation and translocation appear to be coupled kinetically and structurally, as inhibiting tRNA translocation results in impaired CW rotation (Belardinelli et al., 2016; Wasserman et al., 2016).

The finding that EF-G-catalyzed CCW rotation is much faster than tRNA translocation has important consequences for understanding the thermodynamic landscape of translocation. When aa-tRNA has accommodated in the A site and peptide bond formation has taken place, the SSU starts to rotate in the CCW direction driven by thermal energy. At the high cellular EF-G concentrations, the factor is recruited to the ribosome with a rate of >500 s^{-1} (10 μM [EF-G] × 55–150 μM^{-1}s^{-1}; Belardinelli et al., 2016; Katunin et al., 2002), almost instantaneously after EF-Tu has been released. EF-G—presumably in a compact form (Lin et al., 2015)—rapidly binds to either the N or the R state, accelerates CCW rotation on the remaining N complexes to $k_{CCW} = 200$ s^{-1}, and stabilizes the R state by blocking the reverse transitions (Figure 5). Thus, the predicted lifetime of the PRE complex in the N state is negligibly small. Rather, the rotation from N to R is one of the fastest events on the reaction coordinate and is not rate limiting for tRNA-mRNA translocation. After GTP hydrolysis and factor engagement, EF-G promotes translocation by inducing a conformational state of the ribosome in which the body of the SSU starts to move toward the N state, whereas the SSU head swivels further in CCW direction, resulting in ribosome

unlocking (Belardinelli et al., 2016; Wasserman et al., 2016). The unlocking step (40 s^{-1}) (Belardinelli et al., 2016) kinetically dominates both the tRNA movement and release of Pi from EF-G (Savelsbergh et al., 2003). The subsequent Pi release and tRNA movement from the A to P and P to E sites are rapid reactions (Savelsbergh et al., 2003) but may entail additional intermediates that can be isolated by blocking translocation with antibiotics, mutations in EF-G or a lack of GTP hydrolysis (Holtkamp et al., 2014; Pan et al., 2007; Zhou et al., 2014). At this stage, the SSU head and body both move in a CW direction. The E-site tRNA then moves away from the E site at a rate of 14 s^{-1} through at least one additional intermediate state and then dissociates from the ribosome (Belardinelli et al., 2016; Wasserman et al., 2016). The head and the body of the SSU continue to move backward until EF-G dissociates from the ribosome in a relatively slow reaction of ~4 s^{-1} which also completes the re-locking of the ribosome (Belardinelli et al., 2016); this process may entail additional intermediates or conformational varieties of the POST state (Wasserman et al., 2016). All these movements are controlled by the interplay among the tRNAs, EF-G, and GTP hydrolysis. Thus, although the ribosome is a very large particle, movements of its parts are rapid, spontaneous, and driven by thermal energy. Translocation is gated by the ribosome ligands, tRNAs, and EF-G, which control the conformational state of the ribosome, maintain the reading frame, and promote directional movement of the ribosome along the mRNA.

EXPERIMENTAL PROCEDURES

Experiments were carried out in TAKM$_7$ buffer (50 mM Tris-HCl [pH 7.5 at 37°C], 70 mM NH$_4$Cl, 30 mM KCl, 7 mM MgCl$_2$) or in smFRET buffer (50 mM Tris-HCl [pH 7.5 at room temperature], 70 mM NH$_4$Cl, 30 mM KCl, 15 mM MgCl$_2$, 1 mM spermidine, and 8 mM putrescine) at 22°C or 37°C as indicated. Materials were prepared as described in Supplemental Experimental Procedures. subunit rotation experiments were carried out in a stopped-flow apparatus (SX-20MV; Applied Photophysics) using double-labeled ribosomes (S6Alexa488-L9Alexa568) (Belardinelli et al., 2016); the complexes were prepared in the same way as for the quench-flow

Table 2. Summary of the Rates for EF-G-Induced Rotation and Translocation

PRE	k_{CCW}, s^{-1}	k_{CW}, s^{-1}	k_{TL}, s^{-1}
TAKM7, 37°C			
fMK	200 ± 20	15 ± 1	12 ± 2
fMV	210 ± 10	11 ± 1	12 ± 2
smFRET Buffer, 22°C			
fMK	14 ± 1	1.2 ± 0.1	1.2 ± 0.1
fMV	12 ± 1	0.5 ± 0.1	0.6 ± 0.1
TAKM$_7$, 25°C			
fMK	50 ± 3	4 ± 1	2 ± 1

See also Figure S4.

experiments. Alexa 488 was excited at 470 nm, and fluorescence of Alexa 568 was monitored after passing through an OG590 cut-off filter (Schott). Initiation complexes and PRE or POST complexes (0.1 μM, final concentration after mixing throughout) were rapidly mixed with Pmn (10 mM), ternary complex (10 μM), or EF-G (4 μM) as indicated. Time courses of peptide bond formation were measured in a quench-flow apparatus (KinTek) at the same conditions as used in the stopped-flow experiments. The reactions were quenched with KOH (0.5 M); peptides were released by alkaline hydrolysis for 45 min at 37°C, analyzed by reversed-phase high-performance liquid chromatography (HPLC) (LiChrospher 100 RP-8, Merck), and quantified by radioactivity counting (Wohlgemuth et al., 2008). smFRET experiments were performed with double-labeled ribosomes (S6Cy5-L9Cy3) in a total internal reflection fluorescence (TIRF) setup as described previously (Adio et al., 2015). Exponential fitting (with or without a delay phase) was performed using
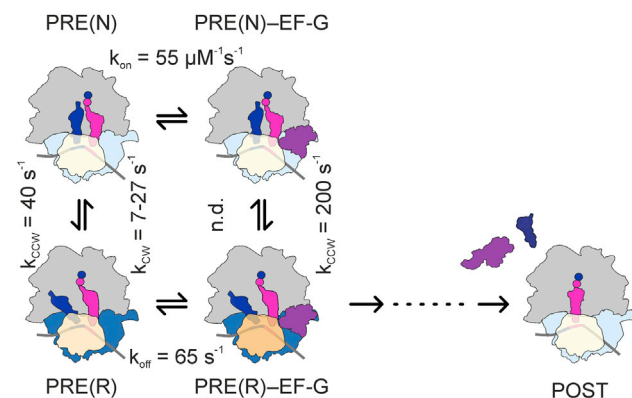
Figure 5. Model for N-to-R Transitions Coupled to the Translocation Pathway

The rotation states of the SSU relative to the LSU (gray) are indicated by color intensity of the SSU body (light blue for N and dark blue for R). The swiveling motions of the SSU head are shown by color gradient from light yellow (classical non-swiveled SSU head position) to orange (swiveled relative to the SSU body) (Belardinelli et al., 2016). tRNAs in the A and P sites of the PRE complex are shown in magenta and blue, respectively. EF-G (purple) is depicted in two conformations: a compact (Lin et al., 2015) and an extended one after engagement with the ribosome and translocation (Ramrath et al., 2013; Zhou et al., 2014). The rates of transitions between PRE(N) and PRE(R), and PRE(N)–EF-G and PRE(R)–EF-G are from this paper. The rates of EF-G binding and dissociation are ensemble rate constants obtained for a mixture of N and R states (Belardinelli et al., 2016) in which the PRE(R) state is predominant (88% for the fMF complex; Table S1). After EF-G recruitment, translocation proceeds through a number of intermediates (see text for details).

GraphPad Prism. Numerical integration analysis was carried out with KinTek Explorer (Johnson et al., 2009).

SUPPLEMENTAL INFORMATION

Supplemental Information includes Supplemental Experimental Procedures, five figures, two tables, and one note and can be found with this article online at http://dx.doi.org/10.1016/j.celrep.2016.07.051.

REFERENCES

Adio, S., Senyushkina, T., Peske, F., Fischer, N., Wintermeyer, W., and Rodnina, M.V. (2015). Fluctuations between multiple EF-G-induced chimeric tRNA states during translocation on the ribosome. Nat. Commun. 6, 7442.

Agirrezabala, X., Lei, J., Brunelle, J.L., Ortiz-Meoz, R.F., Green, R., and Frank, J. (2008). Visualization of the hybrid state of tRNA binding promoted by spontaneous ratcheting of the ribosome. Mol. Cell 32, 190–197.

Aitken, C.E., and Puglisi, J.D. (2010). Following the intersubunit conformation of the ribosome during translation in real time. Nat. Struct. Mol. Biol. 17, 793–800.

Belardinelli, R., Sharma, H., Caliskan, N., Cunha, C.E., Peske, F., Wintermeyer, W., and Rodnina, M.V. (2016). Choreography of molecular movements during ribosome progression along mRNA. Nat. Struct. Mol. Biol. 23, 342–348.

Blanchard, S.C., Kim, H.D., Gonzalez, R.L., Jr., Puglisi, J.D., and Chu, S. (2004). tRNA dynamics on the ribosome during translation. Proc. Natl. Acad. Sci. USA 101, 12893–12898.

Brilot, A.F., Korostelev, A.A., Ermolenko, D.N., and Grigorieff, N. (2013). Structure of the ribosome with elongation factor G trapped in the pretranslocation state. Proc. Natl. Acad. Sci. USA 110, 20994–20999.

Chen, C., Stevens, B., Kaur, J., Cabral, D., Liu, H., Wang, Y., Zhang, H., Rosenblum, G., Smilansky, Z., Goldman, Y.E., and Cooperman, B.S. (2011). Single-molecule fluorescence measurements of ribosomal translocation dynamics. Mol. Cell 42, 367–377.

Chen, J., Petrov, A., Tsai, A., O'Leary, S.E., and Puglisi, J.D. (2013a). Coordinated conformational and compositional dynamics drive ribosome translocation. Nat. Struct. Mol. Biol. 20, 718–727.

Chen, Y., Feng, S., Kumar, V., Ero, R., and Gao, Y.G. (2013b). Structure of EF-G-ribosome complex in a pretranslocation state. Nat. Struct. Mol. Biol. 20, 1077–1084.

Cornish, P.V., Ermolenko, D.N., Noller, H.F., and Ha, T. (2008). Spontaneous intersubunit rotation in single ribosomes. Mol. Cell 30, 578–588.

Cornish, P.V., Ermolenko, D.N., Staple, D.W., Hoang, L., Hickerson, R.P., Noller, H.F., and Ha, T. (2009). Following movement of the L1 stalk between three functional states in single ribosomes. Proc. Natl. Acad. Sci. USA 106, 2571–2576.

Dorner, S., Brunelle, J.L., Sharma, D., and Green, R. (2006). The hybrid state of tRNA binding is an authentic translation elongation intermediate. Nat. Struct. Mol. Biol. 13, 234–241.

Dunkle, J.A., Wang, L., Feldman, M.B., Pulk, A., Chen, V.B., Kapral, G.J., Noeske, J., Richardson, J.S., Blanchard, S.C., and Cate, J.H. (2011). Structures of the bacterial ribosome in classical and hybrid states of tRNA binding. Science 332, 981–984.

Ermolenko, D.N., and Noller, H.F. (2011). mRNA translocation occurs during the second step of ribosomal intersubunit rotation. Nat. Struct. Mol. Biol. 18, 457–462.

Ermolenko, D.N., Majumdar, Z.K., Hickerson, R.P., Spiegel, P.C., Clegg, R.M., and Noller, H.F. (2007a). Observation of intersubunit movement of the ribosome in solution using FRET. J. Mol. Biol. 370, 530–540.

Ermolenko, D.N., Spiegel, P.C., Majumdar, Z.K., Hickerson, R.P., Clegg, R.M., and Noller, H.F. (2007b). The antibiotic viomycin traps the ribosome in an intermediate state of translocation. Nat. Struct. Mol. Biol. 14, 493–497.

Ermolenko, D.N., Cornish, P.V., Ha, T., and Noller, H.F. (2013). Antibiotics that bind to the A site of the large ribosomal subunit can induce mRNA translocation. RNA 19, 158–166.

Fei, J., Kosuri, P., MacDougall, D.D., and Gonzalez, R.L., Jr. (2008). Coupling of ribosomal L1 stalk and tRNA dynamics during translation elongation. Mol. Cell 30, 348–359.

Fei, J., Bronson, J.E., Hofman, J.M., Srinivas, R.L., Wiggins, C.H., and Gonzalez, R.L., Jr. (2009). Allosteric collaboration between elongation factor G and the ribosomal L1 stalk directs tRNA movements during translation. Proc. Natl. Acad. Sci. USA 106, 15702–15707.

Fischer, N., Konevega, A.L., Wintermeyer, W., Rodnina, M.V., and Stark, H. (2010). Ribosome dynamics and tRNA movement by time-resolved electron cryomicroscopy. Nature 466, 329–333.

Frank, J., and Agrawal, R.K. (2000). A ratchet-like inter-subunit reorganization of the ribosome during translocation. Nature 406, 318–322.

Guo, Z., and Noller, H.F. (2012). Rotation of the head of the 30S ribosomal subunit during mRNA translocation. Proc. Natl. Acad. Sci. USA 109, 20391–20394.

Hickerson, R., Majumdar, Z.K., Baucom, A., Clegg, R.M., and Noller, H.F. (2005). Measurement of internal movements within the 30 S ribosomal subunit using Förster resonance energy transfer. J. Mol. Biol. 354, 459–472.

Holtkamp, W., Cunha, C.E., Peske, F., Konevega, A.L., Wintermeyer, W., and Rodnina, M.V. (2014). GTP hydrolysis by EF-G synchronizes tRNA movement on small and large ribosomal subunits. EMBO J. 33, 1073–1085.

Horan, L.H., and Noller, H.F. (2007). Intersubunit movement is required for ribosomal translocation. Proc. Natl. Acad. Sci. USA 104, 4881–4885.

Johnson, K.A., Simpson, Z.B., and Blom, T. (2009). Global kinetic explorer: a new computer program for dynamic simulation and fitting of kinetic data. Anal. Biochem. 387, 20–29.

Joseph, S., and Noller, H.F. (1998). EF-G-catalyzed translocation of anticodon stem-loop analogs of transfer RNA in the ribosome. EMBO J. 17, 3478–3483.

Julián, P., Konevega, A.L., Scheres, S.H., Lázaro, M., Gil, D., Wintermeyer, W., Rodnina, M.V., and Valle, M. (2008). Structure of ratcheted ribosomes with tRNAs in hybrid states. Proc. Natl. Acad. Sci. USA 105, 16924–16927.

Katunin, V.I., Savelsbergh, A., Rodnina, M.V., and Wintermeyer, W. (2002). Coupling of GTP hydrolysis by elongation factor G to translocation and factor recycling on the ribosome. Biochemistry 41, 12806–12812.

Kim, H.D., Puglisi, J.D., and Chu, S. (2007). Fluctuations of transfer RNAs between classical and hybrid states. Biophys. J. 93, 3575–3582.

Li, W., Liu, Z., Koripella, R.K., Langlois, R., Sanyal, S., and Frank, J. (2015). Activation of GTP hydrolysis in mRNA-tRNA translocation by elongation factor G. Sci. Adv. 1, e1500169.

Lin, J., Gagnon, M.G., Bulkley, D., and Steitz, T.A. (2015). Conformational changes of elongation factor G on the ribosome during tRNA translocation. Cell 160, 219–227.

Ling, C., and Ermolenko, D.N. (2015). Initiation factor 2 stabilizes the ribosome in a semirotated conformation. Proc. Natl. Acad. Sci. USA 112, 15874–15879.

Majumdar, Z.K., Hickerson, R., Noller, H.F., and Clegg, R.M. (2005). Measurements of internal distance changes of the 30S ribosome using FRET with multiple donor-acceptor pairs: quantitative spectroscopic methods. J. Mol. Biol. 351, 1123–1145.

Marshall, R.A., Dorywalska, M., and Puglisi, J.D. (2008). Irreversible chemical steps control intersubunit dynamics during translation. Proc. Natl. Acad. Sci. USA 105, 15364–15369.

Moazed, D., and Noller, H.F. (1989). Intermediate states in the movement of transfer RNA in the ribosome. Nature 342, 142–148.

Munro, J.B., Altman, R.B., O'Connor, N., and Blanchard, S.C. (2007). Identification of two distinct hybrid state intermediates on the ribosome. Mol. Cell 25, 505–517.

Munro, J.B., Altman, R.B., Tung, C.S., Cate, J.H., Sanbonmatsu, K.Y., and Blanchard, S.C. (2010a). Spontaneous formation of the unlocked state of the ribosome is a multistep process. Proc. Natl. Acad. Sci. USA 107, 709–714.

Munro, J.B., Altman, R.B., Tung, C.S., Sanbonmatsu, K.Y., and Blanchard, S.C. (2010b). A fast dynamic mode of the EF-G-bound ribosome. EMBO J. 29, 770–781.

Munro, J.B., Wasserman, M.R., Altman, R.B., Wang, L., and Blanchard, S.C. (2010c). Correlated conformational events in EF-G and the ribosome regulate translocation. Nat. Struct. Mol. Biol. 17, 1470–1477.

Pan, D., Kirillov, S.V., and Cooperman, B.S. (2007). Kinetically competent intermediates in the translocation step of protein synthesis. Mol. Cell 25, 519–529.

Qin, P., Yu, D., Zuo, X., and Cornish, P.V. (2014). Structured mRNA induces the ribosome into a hyper-rotated state. EMBO Rep. 15, 185–190.

Ramrath, D.J., Lancaster, L., Sprink, T., Mielke, T., Loerke, J., Noller, H.F., and Spahn, C.M. (2013). Visualization of two transfer RNAs trapped in transit during elongation factor G-mediated translocation. Proc. Natl. Acad. Sci. USA 110, 20964–20969.

Ratje, A.H., Loerke, J., Mikolajka, A., Brünner, M., Hildebrand, P.W., Starosta, A.L., Dönhöfer, A., Connell, S.R., Fucini, P., Mielke, T., et al. (2010). Head swivel on the ribosome facilitates translocation by means of intra-subunit tRNA hybrid sites. Nature 468, 713–716.

Rodnina, M.V., Savelsbergh, A., Katunin, V.I., and Wintermeyer, W. (1997). Hydrolysis of GTP by elongation factor G drives tRNA movement on the ribosome. Nature 385, 37–41.

Savelsbergh, A., Katunin, V.I., Mohr, D., Peske, F., Rodnina, M.V., and Wintermeyer, W. (2003). An elongation factor G-induced ribosome rearrangement precedes tRNA-mRNA translocation. Mol. Cell 11, 1517–1523.

Semenkov, Y.P., Rodnina, M.V., and Wintermeyer, W. (2000). Energetic contribution of tRNA hybrid state formation to translocation catalysis on the ribosome. Nat. Struct. Biol. 7, 1027–1031.

Sievers, A., Beringer, M., Rodnina, M.V., and Wolfenden, R. (2004). The ribosome as an entropy trap. Proc. Natl. Acad. Sci. USA 101, 7897–7901.

Spiegel, P.C., Ermolenko, D.N., and Noller, H.F. (2007). Elongation factor G stabilizes the hybrid-state conformation of the 70S ribosome. RNA 13, 1473–1482.

Valle, M., Zavialov, A., Sengupta, J., Rawat, U., Ehrenberg, M., and Frank, J. (2003). Locking and unlocking of ribosomal motions. Cell 114, 123–134.

Walker, S.E., Shoji, S., Pan, D., Cooperman, B.S., and Fredrick, K. (2008). Role of hybrid tRNA-binding states in ribosomal translocation. Proc. Natl. Acad. Sci. USA 105, 9192–9197.

Wang, L., Altman, R.B., and Blanchard, S.C. (2011). Insights into the molecular determinants of EF-G catalyzed translocation. RNA 17, 2189–2200.

Wasserman, M.R., Alejo, J.L., Altman, R.B., and Blanchard, S.C. (2016). Multi-perspective smFRET reveals rate-determining late intermediates of ribosomal translocation. Nat. Struct. Mol. Biol. 23, 333–341.

Wohlgemuth, I., Brenner, S., Beringer, M., and Rodnina, M.V. (2008). Modulation of the rate of peptidyl transfer on the ribosome by the nature of substrates. J. Biol. Chem. 283, 32229–32235.

Wohlgemuth, I., Pohl, C., and Rodnina, M.V. (2010). Optimization of speed and accuracy of decoding in translation. EMBO J. 29, 3701–3709.

Zhang, W., Dunkle, J.A., and Cate, J.H. (2009). Structures of the ribosome in intermediate states of ratcheting. Science 325, 1014–1017.

Zhou, J., Lancaster, L., Donohue, J.P., and Noller, H.F. (2013). Crystal structures of EF-G-ribosome complexes trapped in intermediate states of translocation. Science 340, 1236086.

Zhou, J., Lancaster, L., Donohue, J.P., and Noller, H.F. (2014). How the ribosome hands the A-site tRNA to the P site during EF-G-catalyzed translocation. Science 345, 1188–1191.

Supplemental Information
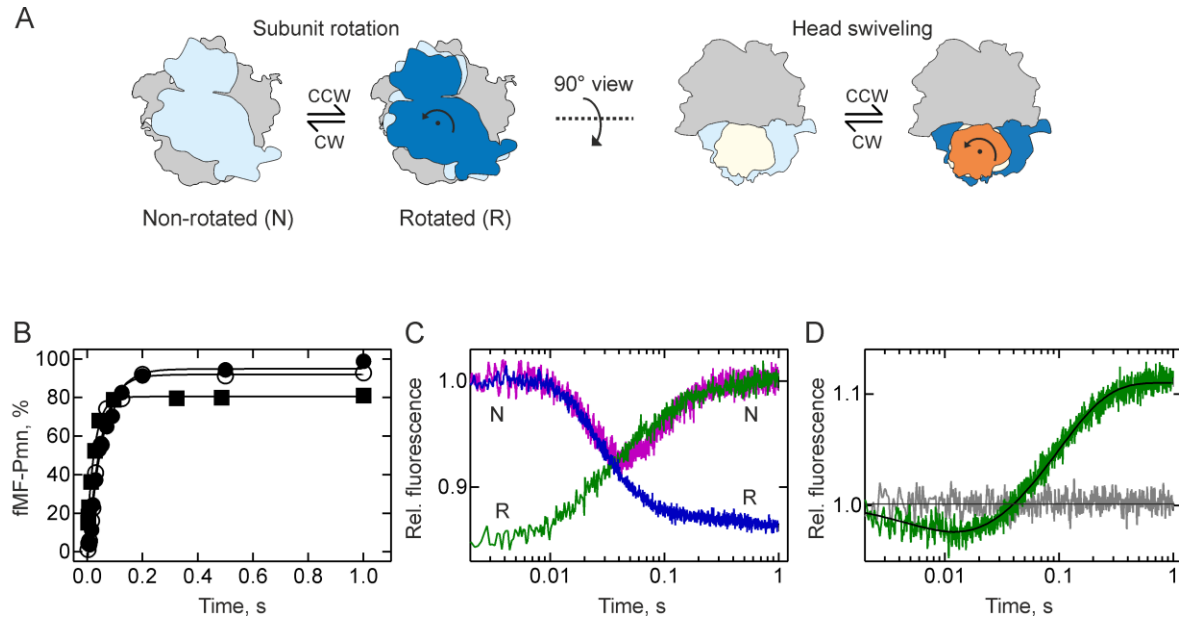
Kinetics of Spontaneous and EF-G-Accelerated

Rotation of Ribosomal Subunits

Heena Sharma, Sarah Adio, Tamara Senyushkina, Riccardo Belardinelli, Frank Peske, and Marina V. Rodnina

Figure S1. Characterization of bS6-bL9 Double-Labeled Ribosomes, Related to Figure 1

(A) Dynamic modes of subunit motions. The rotation states of the SSU relative to the LSU (gray) are indicated by color intensity of the SSU body (light blue for N, dark blue for R). The swiveling motions of the SSU head are shown by color change from light yellow (classical non-swiveled SSU head position) to orange (maximum degree of swiveling relative to the SSU body).

(B) Time resolved Pmn assay for the wild type (closed circle), labeled (S6Alexa488-L9Alexa568) (open circles) and labeled (S6Cy5-L9Cy3) (closed squares) ribosomes.

(C) FRET changes (monitored by fluorescence change of acceptor) upon addition of the ternary complex EF-Tu–GTP–Phe-tRNA^{Phe} to the initiation complex 70S–mRNA–fMet-tRNA^{fMet}, which results in the formation of the PRE complex in the rotated state (blue). Addition of EF-G to the rotated PRE complex forms the POST complex (green). Initiation complex was mixed with ternary complex and EF-G together (pink).

(D) FRET change in the PRE(fMV) complex upon addition of EF-G and translocation (green) or upon mixing with buffer in the absence of EF-G (grey).
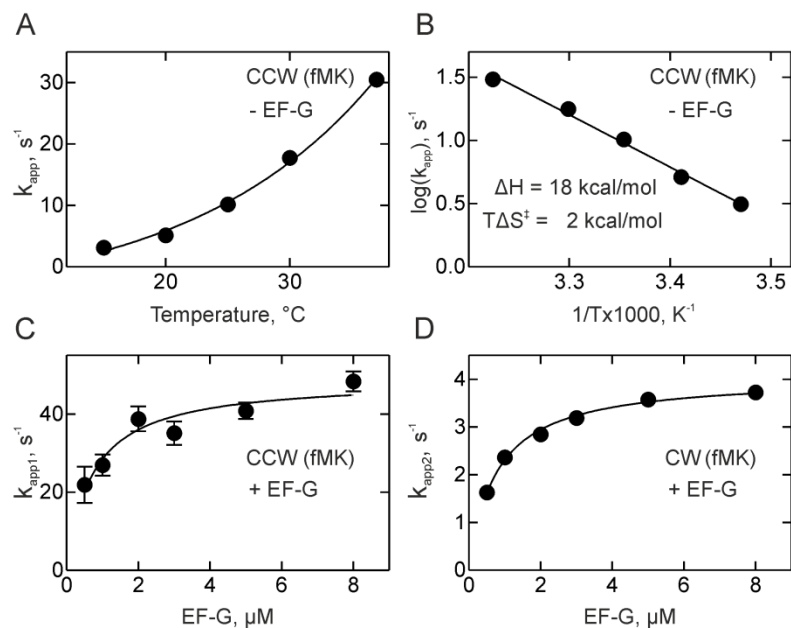
Figure S2. Temperature Dependence of Subunit Rotation, Related to Figures 1 and 4 and Tables 2 and S1

(A and B) Temperature dependence of the spontaneous CCW subunit rotation upon reaction of fMK with Pmn.
(C and D) EF-G concentration dependence of the apparent rate constants of subunit rotation for PRE(fMK) at 25°C. Hyperbolic fits saturate for the CCW rotation at $k_{app1} = 50 \pm 3$ s^{-1} with K_M of 0.7 ± 0.2 μM and for the CW rotation at $k_{app2} = 4.0 \pm 0.1$ s^{-1} with K_M of 0.8 ± 0.1 μM. Error bars are mean values with s.e.m. of the fit.
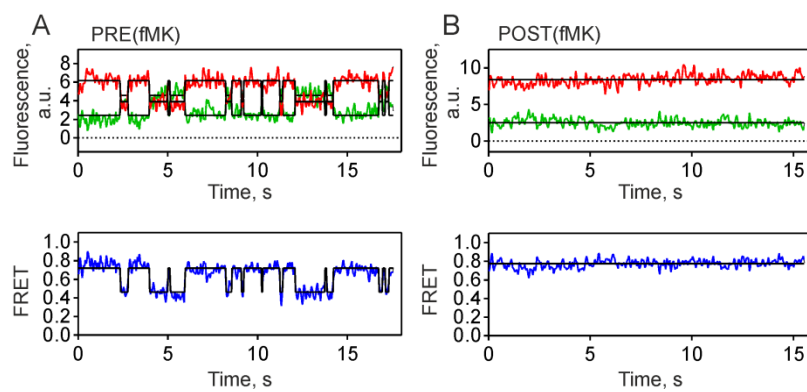
Figure S3. smFRET in the PRE(fMK) Complex, Related to Figure 3 and Tables 1 and Table S1

Representative examples of single-molecule fluorescence intensity trajectories for Cy3 (green) and Cy5 (red) (top panel), and the trajectory of FRET over time (lower panel) (A) in PRE complex and (B) in POST complex
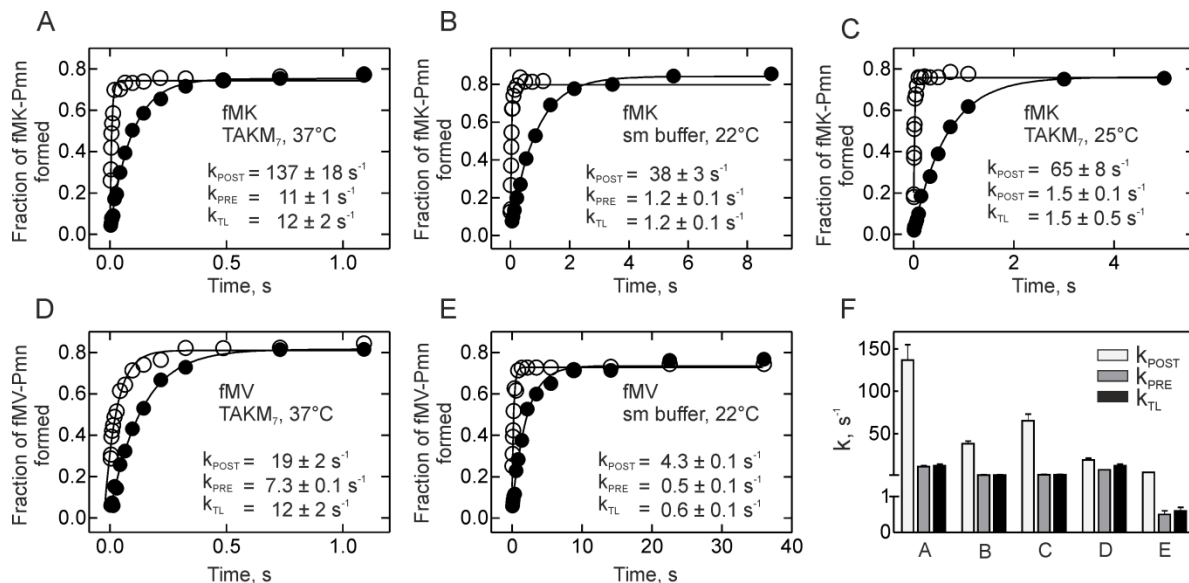
Figure S4. Time-Resolved Pmn Reaction to Determine the Rate of Translocation, **Related to Figure 4 and Table 2**

Open symbols, Pmn reaction with POST complexes; closed symbols, Pmn reaction with PRE complexes upon addition of EF-G. Reaction rates in the POST and PRE complexes were estimated by exponential fitting. k_{TL} was calculated from k_{POST} and k_{PRE} as described in Supplemental Experimental Procedures.

(A) fMK complexes in $TAKM_7$ at 37°C.

(B) fMK complexes in smFRET buffer at 22°C.

(C) fMK complexes in $TAKM_7$ at 25°C.

(D) fMV complexes in $TAKM_7$ at 37°C.

(E) fMV complexes in smFRET buffer at 22°C.

(F) Summary of the rate constants from panels A-E.
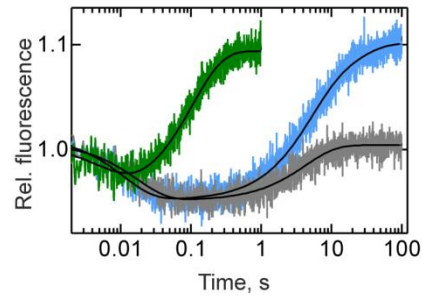
Figure S5. Role of GTP Hydrolysis, Related to Figure 4

FRET change upon reaction of PRE(fMV) complex with EF-G–GTP (green), EF-G–GTPγS (grey), or a mutant EF-G(H583K)–GTP (blue) which is known to be slow in translocation (Savelsbergh et al., 2000).

Table S1. Fraction of N State in PRE Complexes, Related to Figures 3 and 4

PRE	Experimental conditions			
	22°C		25°C	37°C
	smFRET[a]	sm buffer[b]	TAKM$_7$[b]	TAKM$_7$[b]
fMK	0.69 ± 0.03 (512)[c]	0.60 ± 0.04	0.44 ± 0.01	0.41 ± 0.02
fMV	0.60 ± 0.05 (335)[c]	0.57 ± 0.01	n.d.	0.35 ± 0.01
fMF	0.48 ± 0.01 (467)[c]	n.d.	n.d.	0.12 ± 0.03

[a] Determined from the population distribution of smFRET experiment. N is the population in high-FRET state (FRET efficiency = 0.7); R is the population in low-FRET state (FRET efficiency = 0.5).
[b] Calculated from the relative amplitudes of the CCW to CW rotations from ensemble kinetics.
[c] The number of traces used to construct the state distribution histograms.
Values are mean ± s.d. from 3 independent data sets.

Table S2. Spontaneous and EF-G-Induced Transitions in the PRE Complex, Related to Figures 1-4 and Note S1

SUPPLEMENTAL EXPERIMENTAL PROCEDURES

Ribosomes, mRNAs, tRNAs and translation factors

The chromosomal genes for proteins L9 (*rplI*) and S6 (*rpsF*) were deleted in *E. coli* strain BW25113 using the Quick & Easy *E. coli* Gene Deletion Kit (Gene Bridges). The deletion of the genes was confirmed on both the DNA level using gene-specific PCR primers and on the protein level by western blotting and mass spectrometry. Ribosomal subunits were prepared from the deletion strains (ΔL9 and ΔS6) according to the protocol used for native ribosomes (Rodnina and Wintermeyer, 1995). Initiation factors (IF1, IF2, IF3), EF-G, EF-Tu and tRNAs (f[^{3}H]Met-tRNA^{fMet} [^{14}C]Lys-tRNA^{Lys}, [^{14}C]Val-tRNA^{Val}, [^{14}C]Phe-tRNA^{Phe}, [^{14}C]Pro-tRNA^{Pro}) were prepared as described (Cunha et al., 2013a; Holtkamp et al., 2014; Rodnina and Wintermeyer, 1995; Savelsbergh et al., 2003). The following mRNA constructs (IBA, Göttingen) were used (start codon and first elongation codon are underlined).

For stopped-flow experiments and time resolved Pmn assays:
mMK: GUUAACAGGUAUACAUACU<u>AUG</u><u>AAA</u>UUCAUUAC
mMV: GUUAACAGGUAUACAUACU<u>AUG</u><u>GUG</u>UUCAUUAC
mMF: GUUAACAGGUAUACAUACU<u>AUG</u><u>UUU</u>GUUAUUAC
mMP: GGCAAGGAGGUAAAUA<u>AUG</u><u>CCG</u>UUCAUU

For smFRET experiments (mRNAs were biotinylated at the 5' end for attachment to the quartz surface (Adio et al., 2015; Blanchard et al., 2004)):
mMK: CAACCUAAAACUUACACACCCGGCAAGGAGGUAAAUA<u>AUG</u><u>AAG</u>UAAACGAUU
mMV: CAACCUAAAACUUACACACCCGGCAAGGAGGUAAAUA<u>AUG</u><u>GUU</u>UAAACGAUU
mMF: CAACCUAAAACUUACACACCCGGCAAGGAGGUAAAUA<u>AUG</u><u>UUC</u>UAAACGAUU

Labeling of ribosomal subunits

E. coli genes for proteins bL9 and bS6 were PCR-amplified from strain BW25113 and cloned individually into the pET28(a) plasmid (Novagen). Both proteins do not contain native cysteines. For site-specific fluorescence labeling, cysteines were introduced by site-directed mutagenesis at position 41 in protein bS6, replacing aspartic acid, and at position 11 in protein bL9, replacing asparagine. Expression, purification and refolding of proteins were performed essentially as described (Ermolenko et al., 2007; Hickerson et al., 2005; Lieberman et al., 2000). Labeling was performed under denaturing conditions in buffer (50 mM HEPES (pH 7.3), 400 mM KCl, 6 M urea) at 4°C overnight, and the reaction was quenched with 6 mM 2-mercaptoethanol. Excess free dye was removed by gel filtration on a Superdex 75 10/300 GL column (GE Healthcare); the absence of free dye was confirmed by SDS-PAGE. The proteins were refolded by stepwise dialysis into buffer (50 mM HEPES (pH 7.5), 400 mM KCl, 4 mM MgCl$_2$, 5%, v/v, glycerol).

Purified ΔS6 SSU were reconstituted with a 2-fold molar excess of Alexa 488- or Cy5-labeled protein bS6 in buffer (50 mM HEPES (pH 7.5), 400 mM KCl, 20 mM MgCl$_2$, 5%, v/v, glycerol) at 42°C for 60 min. Similarly, purified ΔL9 LSU were reconstituted with a 2-fold molar excess of Alexa 568- or Cy3-labeled protein bL9 in buffer (50 mM HEPES (pH 7.5), 400 mM NH$_4$Cl, 4 mM MgCl$_2$, 5% v/v glycerol) at 37°C for 60 min. Reconstituted subunits were purified by centrifugation through a 30% sucrose cushion in TAKM$_7$ buffer (50 mM Tris-HCl (pH 7.5), 70 mM NH$_4$Cl, 30 mM KCl, 7 mM MgCl$_2$) to remove excess labeled protein. The extent of subunit labeling determined spectroscopically was close to 100%, assuming extinction coefficients of 73,000 cm^{-1}M^{-1} for Alexa 488, 88,000 cm^{-1}M^{-1} for Alexa 568, 150,000 cm^{-1}M^{-1} for Cy3 and 250,000 cm^{-1}M^{-1} for Cy5. Subunit concentrations were determined by absorption measurements at 260 nm on the basis of 67 pmol/A260 unit for SSU and 37 pmol/A260 unit for LSU (Richter, 1976).

Preparation of the complexes

Preparation and purification of initiation, PRE and POST complexes were carried out as described (Belardinelli et al., 2016; Cunha et al., 2013b; Holtkamp et al., 2014; Rodnina et al., 1997). Briefly, labeled SSU were first heat activated in TAKM with 21 mM MgCl$_2$ for 30 min at 37°C, combined with a 1.5-fold excess of labeled LSU and incubated with a 3-fold excess of mRNA and a 2-fold excess of IF1, IF2, IF3 each and a 2.5-fold excess of f[^{3}H]Met-tRNA^{fMet} in TAKM$_7$ buffer containing 1 mM GTP for 30 min at 37°C. Initiation complexes were purified through 1.1 M sucrose cushion in TAKM$_7$. Ternary complexes EF-Tu–GTP–X-tRNA^X (X is Lys, Val, Phe or Pro) were prepared by incubating EF-Tu (2-fold excess over tRNA) with 1 mM GTP, 3 mM phosphophenolpyruvate and 0.1 mg ml^{-1} pyruvate kinase for 15 min at 37°C prior to the addition of aa-tRNA. PRE complex was formed by mixing initiation complexes with a 2-fold excess of ternary complex and incubated for 1 min at 37°C. The resulting

PRE complexes were purified by centrifugation through 1.1 M sucrose cushion in TAKM containing 21 mM $MgCl_2$. The pellets were resuspended in the same buffer and the amount of aa-tRNA binding was measured by nitrocellulose filtration. POST complexes were prepared by adding EF-G (5 nM) to the PRE complexes with 1 mM GTP and incubating for 1 min at 37°C.

Rapid kinetics

Subunit rotation experiments were carried out using a stopped-flow apparatus (SX-20MV; Applied Photophysics) in $TAKM_7$ at 37°C, unless otherwise specified. To monitor subunit rotation we used double-labeled ribosomes (S6Alexa488–L9Alexa568). Alexa 488 was excited at 470 nm and fluorescence of Alexa 568 was monitored after passing through a OG590 cut-off filter (Schott). Spontaneous subunit rotation was monitored by mixing equal volumes of purified POST or initiation complexes (0.1 μM) with either Pmn (10 mM) or ternary complexes (10 μM). Rates of peptide bond formation were measured in a quench-flow apparatus (KinTek). Initiation or POST complexes (0.1 μM) were rapidly mixed with Pmn (10 mM) or ternary complexes (10 μM) and the reaction was quenched with KOH (0.8 M). Peptides were released by alkaline hydrolysis for 45 min at 37°C and analyzed by reversed phase HPLC (LiChrospher 100 RP-8, Merck) and quantified by radioactivity counting (Wohlgemuth et al., 2008).

The concentration dependence of peptide bond formation and the spontaneous subunit rotation with fMK complex (0.1 μM) was performed upon addition of increasing concentrations of Pmn (0.1–20 mM) in either stopped-flow or quench-flow experiments. The temperature dependence of spontaneous subunit rotation was measured with the PRE(fMK) complex (0.1 μM) and Pmn (10 mM) at 15, 20, 25, 30, and 37°C by stopped-flow. Time courses for EF-G-induced subunit rotation were monitored after rapidly mixing PRE complexes (0.05 μM) with EF-G (4 μM) in a stopped-flow apparatus in $TAKM_7$ at 37°C or 25°C, as indicated, or in smFRET buffer (see below) at 22°C. The concentration dependence of subunit rotation for PRE(fMK) and PRE(fMV) (0.05 μM) complexes was monitored with increasing concentration of EF-G (0.5 - 8 μM) in $TAKM_7$ at 37°C and 25°C. Time courses of subunit rotation was also measured with PRE(fMV) complex (0.05 μM) in the presence of EF-G (4 μM) and GTP (1 mM) or GTPγS (1 mM); or EF-G(H583K) (4 μM) and GTP (1 mM) in $TAKM_7$, 37°C.

Time-resolved Pmn assay

The functional activity of ribosome complexes was verified by the time-resolved Pmn assay (Holtkamp et al., 2014). Briefly, fluorescence-labeled or non-labeled PRE(fMF) complexes (0.2 μM final concentration) were rapidly mixed in the quench-flow apparatus with Pmn (10 mM), EF-G (4 μM), and GTP (1 mM). The reaction was quenched with 50% formic acid and samples were treated with 1.5 M sodium acetate saturated with $MgSO_4$. f[^{3}H]Met[^{14}C]Phe-Pmn was extracted into ethyl acetate and quantified by double-label radioactivity counting.

To determine the rate of translocation for PRE(fMK) and PRE(fMV) complexes, PRE or POST complexes (0.2 μM) were mixed with Pmn (10 mM) and EF-G (4 μM) or Pmn (10 mM) in $TAKM_7$ at 37°C, in smFRET buffer at 22°C, or in $TAKM_7$ at 25°C. The reaction was quenched with KOH (0.5 M) and the peptides were released by alkaline hydrolysis for 45 min at 37°C, analyzed by reversed-phase HPLC (LiChrospher 100 RP-8, Merck), and quantified by double-label radioactivity counting (Wohlgemuth et al., 2008). The time required for the PRE complex to react (apparent rate constant k_{PRE}) includes the time needed for translocation ($1/k_{TL}$) and for the Pmn reaction of the resulting POST state ($1/k_{POST}$). Deconvolution of the translocation rate from the two values ($k_{TL} = k_{PRE} \times k_{POST} / (k_{PRE} - k_{POST})$ gives the rate of tRNA translocation (Holtkamp et al., 2014).

Data analysis

Exponential fitting was performed using GraphPad Prism. Time courses of peptide bond formation (**Figures 1A, 1D, 2A, S1B and S4**) were evaluated by single-exponential fitting. Time courses of CCW rotation after the Pmn reaction (**Figures 1B, 1E, S2A and S2B**) were initially evaluated by an equation accounting for one (fMV) or two (fMK, fMF) exponential terms after a delay due to the preceding Pmn reaction. The origin of the minor additional downward phase is unknown; it constituted 12% and 20% of the total signal for fMK and fMF complexes, respectively. The elemental rate of subunit rotation for fMK ($k_{CCW} = 48 \pm 3$ s^{-1}) was calculated from $k_{pep} = 240 \pm 20$ s^{-1} (**Figure 1D**) and $k_{rot} = 40 \pm 1$ s^{-1} (**Figure 1E**) using the equation $k_{CCW} = k_{pep} \times k_{rot} / (k_{pep} - k_{rot})$. Time courses with fMP did not show the delay and were evaluated by two-exponential fitting with the two phases constituting 55% and 45% of the total amplitude change.

Time courses of EF-G-catalyzed subunit rotation with PRE(fMK) and PRE(fMV) (at all conditions) and with PRE(fMF) at smFRET conditions (**Figures 4, S2C and S2D**) were evaluated by two-exponential fitting. From the two exponential fitting of the traces for PRE(fMK) and PRE(fMV) the ratio of the amplitude change for the downward phase (A_1) and upward phase (A_2) was calculated. The downward phase A_1 represents the CCW rotation

on those ribosomes that were in the N state before EF-G addition. The upward phase A_2 provides the full span of the R to N transitions on all ribosomes. Thus, the A_1/A_2 ratio gave the fraction of the ribosome in the N state before EF-G binding.

Numerical integration analysis was carried out with KinTek Explorer (Johnson et al., 2009) using a two- or three-step model, as was required, with all steps irreversible for the traces in **Figures 1A and 1B**. The first two steps describe the formation of the peptide bond and the subsequent the subunit rotation, respectively. We assumed that the subunit rotation is quasi-irreversible at 37°C in $TAKM_7$. The third step is to account for a slow decrease at the end of each stopped-flow trace (see above). From the analysis we obtained the rate constant of peptide bond formation and the elemental rate of subunit rotation as reported in **Figure 1F**. For fMP, numerical integration analysis with a two-step model was unable to deconvolute the steps of subunit rotation and peptide bond formation. The apparent rate constants of the first and the second steps were about 0.2 s^{-1} and 0.03 s^{-1} respectively, which were the same as the rates from exponential fitting, precluding further analysis.

Numerical integration was also performed for the data shown in **Figures 2A–C** using three-step and two-step models (no slow phase was observed for the complexes shown in Figure 2C), respectively. We noted that for POST(fMF) complex **(Figure 2C)**, there was a maximum change in the amplitude for N to R transition upon binding of ternary complex and the final intrinsic florescence intensity (IFI) value was the smallest compared to other complexes **(Figure 2B).** We assumed, in the simplest model, that the endpoint differences between the time courses in **Figure 2B** reflect the difference in the fraction of R states in the final population of ribosomes. We thus fixed the absolute IFI value for the R state to that obtained for the POST(fMF) complex. In the three-step model used for fitting, the first irreversible step accounted for peptide bond formation, the second reversible step was the subunit rotation (CCW and CW), and the third step (where necessary) accounted for the additional minor decrease at the end of each stop-flow trace. All data for PRE(fMK), PRE(fMV) and PRE(fMF) complexes, including quench-flow and stopped-flow time courses were fitted simultaneously (global fit) using the same IFI values for the N and R state independently of tRNAs. Average values of rate constants and standard deviations (s.d.) were calculated from three independent experiments.

Single-molecule FRET

smFRET experiments were carried out in smFRET buffer (50 mM Tris-HCl (pH 7.5), 70 mM NH$_4$Cl, 30 mM KCl, 15 mM MgCl$_2$, 1 mM spermidine and 8 mM putrescine) and data analysis was performed as described (Adio et al., 2015) using double-labeled ribosomes (S6Cy5–L9Cy3). Initiation complexes were formed by incubating ribosomes (0.1 μM) with a 1.7-fold excess of IF1, IF2 and IF3, 3-fold excess of mRNA biotinylated at the 5' end and fMet-tRNA^{fMet}, and GTP (1 mM) in $TAKM_7$ at 37°C for 30 min. Ternary complexes were prepared as described above with EF-Tu (1 μM) and X-tRNA^X (X is Lys, Val, Phe) (0.5 μM). Initiation complexes were mixed with a 5-fold excess of ternary complex and incubated for 1 min at room temperature to form PRE complexes. POST complexes were formed by incubating PRE complexes with EF-G (0.1 μM) and GTP (1 mM).

NOTE S1.

Summary of smFRET and ensemble kinetic data on ribosome fluctuations linked to translocation.

Ribosome dynamics plays a key role in EF-G-catalyzed translocation. Some aspects of ribosome dynamics in translocation are extensively studied and well understood. The most commonly studied motions are rotations of the ribosomal subunits (N to R and R to N), swiveling motions of the SSU head, changes of tRNA positions from classical (C) to hybrid (H) position, and closing of the L1 stalk on the E-site tRNA. These motions can occur spontaneously in the absence of EF-G and are only loosely coupled (Fischer et al., 2010; Munro et al., 2010c; Wasserman et al., 2016). smFRET studies provided important insights into spontaneous ribosome dynamics by looking from several perspectives, i.e., using labels at different positions of the ribosome complex. Due to the variety of reporters, experimental conditions, and differences in ribosome complexes under study, it is sometimes difficult to compare the results of individual papers and assess their relevance for understanding translocation. This Supplemental Note and Table S2 are designed to make this information more accessible.

To classify the available experimental information, we first sort them according to the type of ribosome complexes used in the studies, i.e., PRE complexes, complexes with a vacant A site, or and vacant ribosomes lacking both A- and P-site tRNAs (Table S2). Of these three types of complexes, the experiments with PRE complexes are of immediate relevance for understanding translocation, because the occupancy of the A site is a key prerequisite for the reaction (Joseph and Noller, 1998).

Among the experiments with PRE complexes, we then distinguish three major types of movements, subunit rotation, tRNA repositioning and L1 movement (Table S2, sheet 1, and references therein). The subunit rotation from N to R (CCW) and from R to N (CW) was studied by labels attached to ribosomal proteins S6 and L9 (Cornish et al., 2008; Qin et al., 2014), or helices h44 and H101 (Marshall et al., 2008) on the SSU and LSU, respectively. More recently, subunit rotation has also been monitored using a FRET pair on proteins S13 and L1 and S13 and L5 (Wasserman et al., 2016). We note that the assignment of S13-L1 and S13-L5 dynamics as subunit rotation is not unambiguous, as it may also represent movements of the L1 stalk or the SSU head relative to the body. To study tRNA movements from the C to H and H to C states, different groups utilized labels on the tRNAs in the A and P sites (Adio et al., 2015; Blanchard et al., 2004; Chen et al., 2011; Kim et al., 2007; Munro et al., 2007; Munro et al., 2010a; Wasserman et al., 2016). Additionally, the A-site tRNA movement was monitored by a fluorescence reporter pair attached to the tRNA and protein L11 (Adio et al., 2015; Chen et al., 2011), L27 (Altuntop et al., 2010), and S13 (Wasserman et al., 2016). Finally, L1 closing and opening was visualized by L1-tRNA (Fei et al., 2009; Fei et al., 2008; Munro et al., 2010b), L1-L9 (Fei et al., 2009), and L1-L33 pairs (Cornish et al., 2009; Qin et al., 2014).

Spontaneous ribosome transitions in the absence of EF-G are well characterized. Addition of EF-G induces rapid translocation, which makes it difficult to dissect the effect of the factor on the transitions, because PRE complexes are rapidly converted to the POST state. Several smFRET papers identify translocation intermediates (INT or CHI states) (Adio et al., 2015; Chen et al., 2011; Munro et al., 2007; Wasserman et al., 2016); those are not addressed here and in the following we will summarize what is known about the kinetics of spontaneous ribosome dynamics in the absence of EF-G.

For the SU rotation in the CCW direction measured with the S6-L9 reporter, most k_{CCW} values are between 0.3 s^{-1} and 1.7 s^{-1} (Cornish et al., 2008; Qin et al., 2014); these values compare reasonably well with those determined by us, 2-4 s^{-1} (Table 1). An alternative FRET pair S13-L1 reports on a relatively rapid rearrangement, 4.7 s^{-1}, whereas the S13-L5 pair reports on a slower reaction, about 0.1 s^{-1} (Wasserman et al., 2016). With the S6-L9, S13-L1, and S13-L5 labels, the N to R rotation in the PRE complex is reversible with a rate of CW rotation in the range of 0.02 s^{-1} to 12.7 s^{-1} (this paper Table 1, 22°C, and (Cornish et al., 2008; Qin et al., 2014; Wasserman et al., 2016). Surprisingly, when the labels are attached to rRNA (h44-H101), CCW rotation is very slow (about 0.05 s^{-1}) and quasi irreversible (Marshall et al., 2008). The effect of EF-G on the subunit rotation of the PRE complex has not been reported previously, because EF-G addition facilitates rapid formation of translocation intermediates followed by translocation (Wasserman et al., 2016).

Experiments monitoring C-to-H tRNA transitions provide a similar kinetic picture. The rates of C-to-H transitions $k_{C \rightarrow H}$ are in the range from 0.6 to 10 s^{-1} and are reversible with $k_{H \rightarrow C}$ between 0.7 and 4 s^{-1}, and a resulting ratio between H and C states ranging from 0.2 to 2 (Adio et al., 2015; Altuntop et al., 2010; Blanchard et al., 2004; Chen et al., 2011; Kim et al., 2007; Munro et al., 2007; Munro et al., 2010a; Wasserman et al., 2016). Again, the effect of EF-G on the C-to-H transition is difficult to assess, because EF-G induces rapid formation of translocation intermediates that differ from the initial H and C states (Adio et al., 2015; Chen et al., 2011; Wasserman et al., 2016).

Probably the most studied transition is the movement of protein L1 towards or away from the E-site tRNA, which we define as open-to-closed transition. Most of the estimated closing rates $k_{L1open \rightarrow closed}$ are around 2-5 s^{-1} (Cornish et al., 2009; Fei et al., 2009; Munro et al., 2010a; Munro et al., 2010c). The rates of opening $k_{L1open \rightarrow closed}$ are from 0.4 s^{-1} (Cornish et al., 2009) to as high as 46 s^{-1} (Munro et al., 2010c); in the latter case the high observed rate may reflect the existence of intermediates. EF-G addition results in rapid translocation (Fei et al., 2008). In one case, fluctuations between open and closed L1 conformations were observed after EF-G addition and the rate of these transitions was not changed compared to spontaneous transitions in the absence of EF-G (Munro et al., 2010c). However, the exact timing of EF-G arrival to the ribosomes in those experiments remained unclear and it is difficult to rule out a possibility that the observed unaltered fluctuations represent ribosome dynamics in the absence of EF-G. In summary, smFRET measurements suggests that in the PRE complex N to R, C to H and L1 open to closed transitions are spontaneous and reversible, loosely coupled and thermodynamically driven and the effect of EF-G on the rate of these transitions is not clear.

Because the effect of EF-G on PRE complexes is elusive and difficult to resolve, several studies addressed EF-G-induced ribosome dynamics with complexes that lacked a tRNA in the A site or with vacant ribosomes lacking tRNAs in both A and P sites (Table S2, sheet 2). The dynamics of vacant ribosomes or ribosomes with a peptidyl-tRNA in the P site was very slow (Cornish et al., 2008). For the complexes with a vacant A site and a deacylated tRNA in the P site, the rates of fluctuations are similar to those on PRE complexes. The reported acceleration effect of EF-G on the ribosome rotation (measured with S6-L9 pair) was two-fold (Cornish et al., 2008), and on L1 closure six- to eight-fold (Fei et al., 2009; Munro et al., 2010b). Because of the lack of the A-site tRNA, which is essential for translocation (Joseph and Noller, 1998), it is unclear whether these results pertain to the situation during on-going translocation, particularly in view of the absence of the EF-G effect on PRE complexes. We note that despite a large eight-fold effect of EF-G–GDPNP binding on the rate of L1 closure, the authors concluded that EF-G does not accelerate the formation of the R–H–L1$_{closed}$ state (Munro et al., 2010b). In general, the rates obtained by smFRET are significantly slower than those estimated by ensemble kinetics (Table S2, sheet 3). On the other hand, the rate of spontaneous subunit rotation was not measured by ensemble kinetics. This summary illustrates that the effect of EF-G on the subunit rotation prior to translocation is not known, despite a wealth of information on the ribosome dynamics obtained by smFRET.

SUPPLEMENTAL REFERENCES

Adio, S., Senyushkina, T., Peske, F., Fischer, N., Wintermeyer, W., and Rodnina, M.V. (2015). Fluctuations between multiple EF-G-induced chimeric tRNA states during translocation on the ribosome. Nat Commun *6*, 7442.

Altuntop, M.E., Ly, C.T., and Wang, Y. (2010). Single-molecule study of ribosome hierarchic dynamics at the peptidyl transferase center. Biophys J *99*, 3002-3009.

Belardinelli, R., Sharma, H., Caliskan, N., Cunha, C.E., Peske, F., Wintermeyer, W., and Rodnina, M.V. (2016). Choreography of molecular movements during ribosome progression along mRNA. Nat Struct Mol Biol *23*, 342-348.

Blanchard, S.C., Kim, H.D., Gonzalez, R.L., Jr., Puglisi, J.D., and Chu, S. (2004). tRNA dynamics on the ribosome during translation. Proc Natl Acad Sci U S A *101*, 12893-12898.

Chen, C., Stevens, B., Kaur, J., Cabral, D., Liu, H., Wang, Y., Zhang, H., Rosenblum, G., Smilansky, Z., Goldman, Y.E.*, et al.* (2011). Single-molecule fluorescence measurements of ribosomal translocation dynamics. Mol Cell *42*, 367-377.

Cornish, P.V., Ermolenko, D.N., Noller, H.F., and Ha, T. (2008). Spontaneous intersubunit rotation in single ribosomes. Mol Cell *30*, 578-588.

Cornish, P.V., Ermolenko, D.N., Staple, D.W., Hoang, L., Hickerson, R.P., Noller, H.F., and Ha, T. (2009). Following movement of the L1 stalk between three functional states in single ribosomes. Proc Natl Acad Sci U S A *106*, 2571-2576.

Cunha, C.E., Belardinelli, R., Peske, F., Holtkamp, W., Wintermeyer, W., and Rodnina, M.V. (2013b). Dual use of GTP hydrolysis by elongation factor G on the ribosome. Translation *1*, e24315.

Ermolenko, D.N., Majumdar, Z.K., Hickerson, R.P., Spiegel, P.C., Clegg, R.M., and Noller, H.F. (2007). Observation of intersubunit movement of the ribosome in solution using FRET. J Mol Biol *370*, 530-540.

Fei, J., Bronson, J.E., Hofman, J.M., Srinivas, R.L., Wiggins, C.H., and Gonzalez, R.L., Jr. (2009). Allosteric collaboration between elongation factor G and the ribosomal L1 stalk directs tRNA movements during translation. Proc Natl Acad Sci U S A *106*, 15702-15707.

Fei, J., Kosuri, P., MacDougall, D.D., and Gonzalez, R.L., Jr. (2008). Coupling of ribosomal L1 stalk and tRNA dynamics during translation elongation. Mol Cell *30*, 348-359.

Fischer, N., Konevega, A.L., Wintermeyer, W., Rodnina, M.V., and Stark, H. (2010). Ribosome dynamics and tRNA movement by time-resolved electron cryomicroscopy. Nature *466*, 329-333.

Hickerson, R., Majumdar, Z.K., Baucom, A., Clegg, R.M., and Noller, H.F. (2005). Measurement of internal movements within the 30 S ribosomal subunit using Forster resonance energy transfer. J Mol Biol *354*, 459-472.

Holtkamp, W., Cunha, C.E., Peske, F., Konevega, A.L., Wintermeyer, W., and Rodnina, M.V. (2014). GTP hydrolysis by EF-G synchronizes tRNA movement on small and large ribosomal subunits. EMBO J *33*, 1073-1085.

Johnson, K.A., Simpson, Z.B., and Blom, T. (2009). Global kinetic explorer: a new computer program for dynamic simulation and fitting of kinetic data. Anal Biochem *387*, 20-29.

Joseph, S., and Noller, H.F. (1998). EF-G-catalyzed translocation of anticodon stem-loop analogs of transfer RNA in the ribosome. EMBO J *17*, 3478-3483.

Kim, H.D., Puglisi, J.D., and Chu, S. (2007). Fluctuations of transfer RNAs between classical and hybrid states. Biophys J *93*, 3575-3582.

Lieberman, K.R., Firpo, M.A., Herr, A.J., Nguyenle, T., Atkins, J.F., Gesteland, R.F., and Noller, H.F. (2000). The 23 S rRNA environment of ribosomal protein L9 in the 50 S ribosomal subunit. J Mol Biol *297*, 1129-1143.

Marshall, R.A., Dorywalska, M., and Puglisi, J.D. (2008). Irreversible chemical steps control intersubunit dynamics during translation. Proc Natl Acad Sci U S A *105*, 15364-15369.

Munro, J.B., Altman, R.B., O'Connor, N., and Blanchard, S.C. (2007). Identification of two distinct hybrid state intermediates on the ribosome. Mol Cell *25*, 505-517.

Munro, J.B., Altman, R.B., Tung, C.S., Cate, J.H., Sanbonmatsu, K.Y., and Blanchard, S.C. (2010a). Spontaneous formation of the unlocked state of the ribosome is a multistep process. Proc Natl Acad Sci U S A *107*, 709-714.

Munro, J.B., Altman, R.B., Tung, C.S., Sanbonmatsu, K.Y., and Blanchard, S.C. (2010b). A fast dynamic mode of the EF-G-bound ribosome. EMBO J *29*, 770-781.

Munro, J.B., Wasserman, M.R., Altman, R.B., Wang, L., and Blanchard, S.C. (2010c). Correlated conformational events in EF-G and the ribosome regulate translocation. Nat Struct Mol Biol *17*, 1470-1477.

Qin, P., Yu, D., Zuo, X., and Cornish, P.V. (2014). Structured mRNA induces the ribosome into a hyper-rotated state. EMBO Rep *15*, 185-190.

Richter, D. (1976). Stringent factor from Escherichia coli directs ribosomal binding and release of uncharged tRNA. Proc Natl Acad Sci U S A *73*, 707-711.

Rodnina, M.V., Savelsbergh, A., Katunin, V.I., and Wintermeyer, W. (1997). Hydrolysis of GTP by elongation factor G drives tRNA movement on the ribosome. Nature *385*, 37-41.

Rodnina, M.V., and Wintermeyer, W. (1995). GTP consumption of elongation factor Tu during translation of heteropolymeric mRNAs. Proc Natl Acad Sci U S A *92*, 1945-1949.

Savelsbergh, A., Katunin, V.I., Mohr, D., Peske, F., Rodnina, M.V., and Wintermeyer, W. (2003). An elongation factor G-induced ribosome rearrangement precedes tRNA-mRNA translocation. Mol Cell *11*, 1517-1523.

Savelsbergh, A., Matassova, N.B., Rodnina, M.V., and Wintermeyer, W. (2000). Role of domains 4 and 5 in elongation factor G functions on the ribosome. J Mol Biol *300*, 951-961.

Wasserman, M.R., Alejo, J.L., Altman, R.B., and Blanchard, S.C. (2016). Multiperspective smFRET reveals rate-determining late intermediates of ribosomal translocation. Nat Struct Mol Biol *23*, 333-341.

Wohlgemuth, I., Brenner, S., Beringer, M., and Rodnina, M.V. (2008). Modulation of the rate of peptidyl transfer on the ribosome by the nature of substrates. J Biol Chem *283*, 32229-32235.